



ANNUAL RESEARCH REPORT

2019

Gary S. Was, Director
Ovidiu Toader, Manager and Research Specialist
Fabian Naab, Research Specialist
Ethan Uberseder, Research Specialist
Thomas Kubley, Research Engineer

2600 Draper Road
Department of Nuclear Engineering and Radiological Sciences
University of Michigan
Ann Arbor, Michigan 48109-2145
mibl.engin.umich.edu

Telephone: (734) 936-0131

Fax: (734) 763-4540

The Annual Research Report

This report summarizes the principal research activities in the Michigan Ion Beam Laboratory during the past calendar year. One hundred and seven researchers conducted 40 projects at MIBL that accounted for 180 irradiations and 5040 hours of instrument usage. The programs included participation from researchers at the University, corporate research laboratories, private companies, government laboratories, and other universities across the United States. These projects also included 6 projects funded through the Nuclear Science User Facility program. The extent of participation of the laboratory in these programs ranged from routine surface analysis to ion assisted film formation. Experiments included Rutherford backscattering spectrometry, elastic recoil spectroscopy, nuclear reaction analysis, direct ion implantation, ion beam mixing, ion beam assisted deposition, and radiation damage by proton bombardment. The following pages contain a synopsis of the research conducted in the Michigan Ion Beam Laboratory during the 2018 calendar year.

About the Laboratory

The Michigan Ion Beam Laboratory for Surface Modification and Analysis was completed in October of 1986. The laboratory was established for the purpose of advancing our understanding of ion-solid interactions by providing up-to-date equipment with unique and extensive facilities to support research at the cutting edge of science. Researchers from the University of Michigan as well as industry and other universities are encouraged to participate in this effort.

The lab houses a 3 MV Pelletron accelerator, a 1.7 MV tandem ion accelerator, and a 400 kV ion implanter that are configured to provide for a range of ion irradiation and ion beam analysis capabilities. The control of the parameters and the operation of these systems are mostly done by computers and are interconnected through a local area network, allowing for complete control of irradiations from the control room as well as off-site monitoring and control.

In 2010, MIBL became a Partner Facility of the National Scientific User Facility (NSUF), based at Idaho National Laboratory, providing additional opportunities for researchers across the US to access the capabilities of the laboratory. In 2016, MIBL was recognized as the top ion beam laboratory in the U.S. by the Nuclear Science User Facilities program.

This past year, beam lines 6 and 8 were fabricated and connected to the newly installed 300 kV FEI Tecnai G2 TEM to provide the capability to conduct in-situ irradiation with simultaneous He implantation. Both beams have been brought into the TEM and the facility will be ready for users in early 2019.

Respectfully submitted,



Gary S. Was, Director

Research Projects

Nuclear Science User Facility (NSUF) Projects

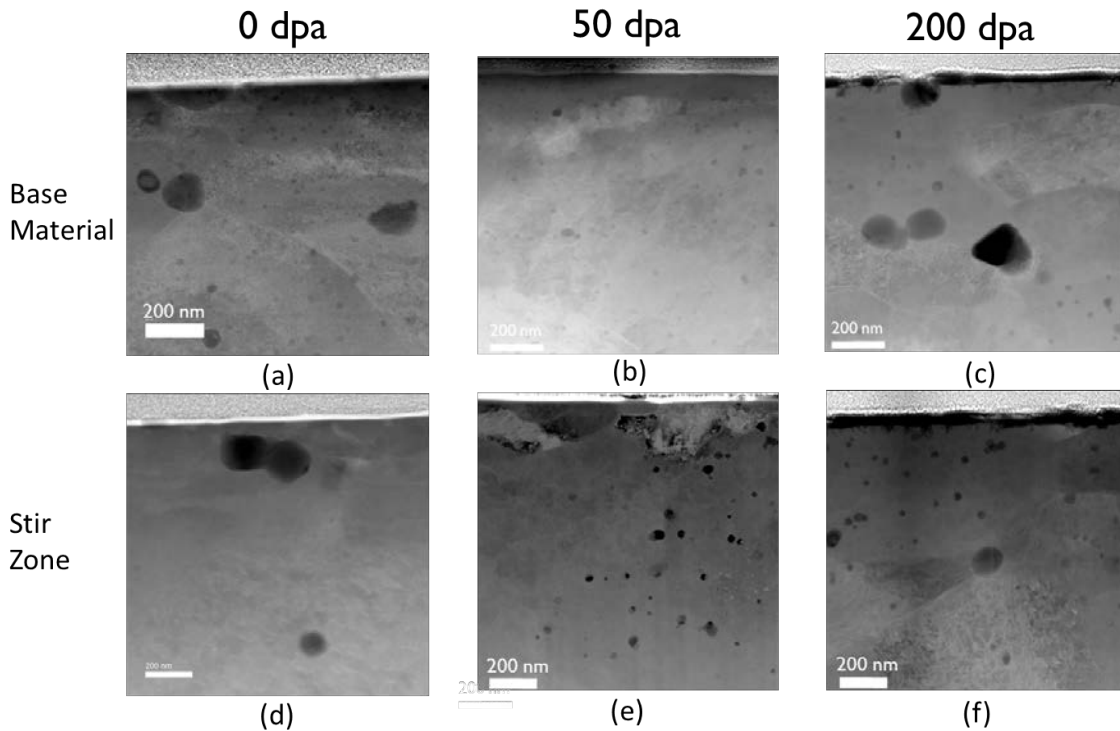
IRRADIATION EFFECTS IN WELDED ODS STEELS AT HIGH DOSE

E. Getto, B. Baker

Department of Mechanical Engineering, United States Naval Academy

Determining the microstructural behavior of oxide dispersion strengthened (ODS) alloys is important for predicting the safety and structural integrity of fast reactors. Furthermore, the behavior of welds in reactors is a significant concern as welds are a weak point in terms of mechanical properties. Self-ion irradiation experiments have been performed on welded and as received alloys MA956 to determine the microstructure response to irradiation at 400, 450 and 500°C up to 200 displacements per atom (dpa). Irradiations were performed with 5 MeV Fe^{++} ions on samples using a raster-scanned beam from the 1.7 MV Tandatron accelerator in the Michigan Ion Beam Laboratory. The effects of friction stir welding (with varying heat inputs) were determined using an Analytical Electron Microscope in scanning transmission electron microscopy (STEM) mode and atom probe tomography (APT) to determine precipitate behavior.

This work was supported by NSUF RTE 17-1032.



Microstructure of base material and welding stir zone in ODS alloy in MA956 imaged using STEM in the HAADF (high angle annular dark field) at 450°C.

FISSION PRODUCT TRANSPORT IN SiC UNDER IRRADIATION

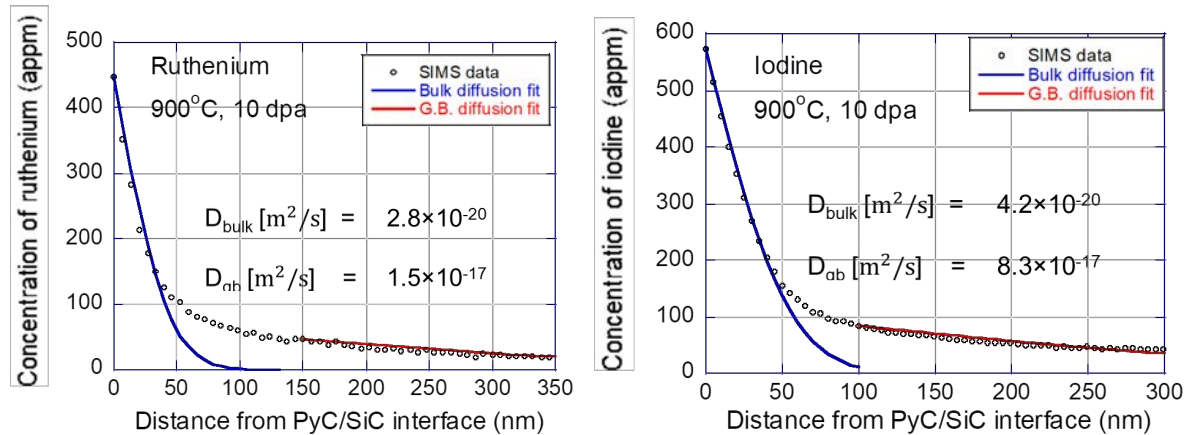
Z. Jiao, R. Wahlen, Q. Peng, N. Chen, F. Gao, G.S. Was

Department of Nuclear Engineering and Radiological Sciences, University of Michigan

The objective of this research is to measure diffusion coefficients of fission products (FPs) in SiC under irradiation conditions, as well as synergistic effects of radiation damage, and fission product behavior at the IPyC/SiC interface. Molecular dynamics simulations are used to validate experimental data and determine the atomistic diffusion mechanisms to further improve empirical models used in the PARFUME code to predict FP release in TRISO fuel.

SiC-PyC-SiC diffusion couples were pre-implanted with iodine or ruthenium in the PyC layer. The diffusion couples were then subject to 4.8 MeV silicon ion irradiation at 900°C to 10 dpa using the accelerator Blue in the Michigan Ion Beam Laboratory. Distribution of iodine and ruthenium in the diffusion couples after ion irradiation was characterized using secondary ion mass spectrometry (SIMS) at Surface Science Western, University of Western Ontario. I and Ru were found to pile up at the SiC cap/PyC interface, the PyC/SiC interfaces as well as into the bulk SiC. FP diffusion in bulk SiC should proceed via two different mechanisms: bulk or grain boundary diffusion. When both bulk and grain boundary diffusion are significant for the overall FP flux, the bulk diffusion concentration profile follows the Fickian analysis while the grain boundary diffusion tail, which has a source term composed of the interface concentration and the bulk diffusion front, requires a complicated analysis to calculate a diffusion coefficient. The bulk and grain boundary diffusivities of Ru in SiC under ion irradiation are determined to be $2.8 \times 10^{-20} \text{ m}^2/\text{s}$ and $1.5 \times 10^{-17} \text{ m}^2/\text{s}$, respectively. The bulk and grain boundary diffusivities of I in SiC under ion irradiation are $4.2 \times 10^{-20} \text{ m}^2/\text{s}$ and $8.3 \times 10^{-17} \text{ m}^2/\text{s}$, respectively. Iodine and ruthenium have comparable bulk and grain boundary diffusivities. The data fitting for Ru and I is shown in figures.

Support of this work was provided by DOE NEUP and NSUF under award # DE-NE0008519.



SIMS data fit used to calculate the diffusivities of ruthenium and iodine through the bulk and along grain boundaries.

USING ION IRRADIATION TO EXTEND THE DAMAGE LEVEL OF NEUTRON IRRADIATED STAINLESS STEELS

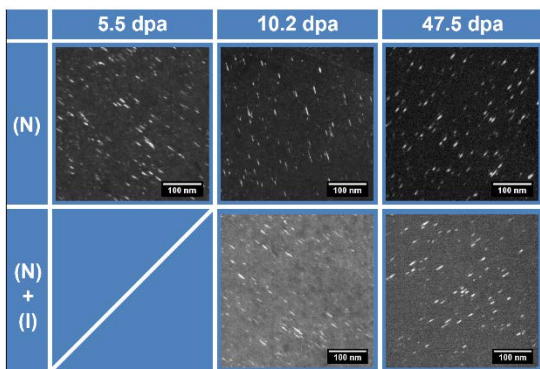
S. Levine, Z. Jiao, G.S. Was

Department of Nuclear Engineering and Radiological Sciences, University of Michigan

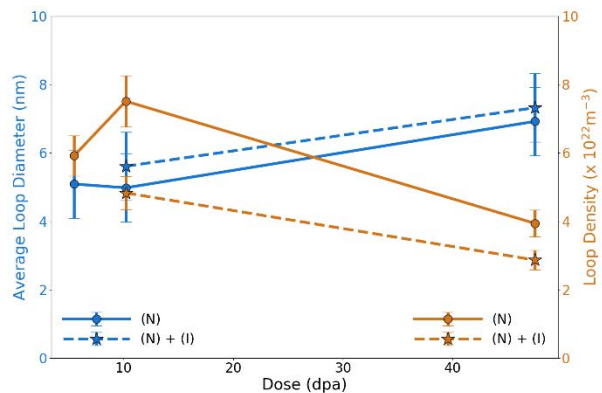
As the United States' light water reactor fleet continues to age, many plants are applying for license renewal. For regulators and plant operators, structural material degradation is a chief concern. While ion irradiation is a useful tool to predict future material degradation, resulting microstructures are extremely sensitive to initial composition and heat treatment. Unfortunately, archive material of the same heat already being used in reactor is rarely available. Thus, the objective of this study is to determine the efficacy of irradiating neutron irradiated material (preconditioned samples) with heavy ions to simulate high dpa level damage.

In order to replicate neutron radiation damage with heavy ions at high damage rates, there must be an adequate shift in temperature so that the flux of point defects to sinks or the number of point defects that recombine is invariant (Mansur 1978). The studies that were performed at the Michigan Ion Beam Laboratory with the 3 MV accelerator Wolverine were used to identify the appropriate temperature shift for 9 MeV Ni³⁺ irradiations at a dose rate of ~10⁻³ dpa/s where the material of interest was 304L stainless steel previously irradiated in the BOR-60 fast reactor at 320°C at a dose rate of 9.4 x 10⁻⁷ dpa/s (E > 0.1 MeV). Irradiations were conducted at 380°C, 400°C, and 420°C to add 42 dpa of damage to samples preconditioned with 5.5 dpa neutron damage. The samples that were ion+neutron irradiated were compared to samples from the BOR-60 reactor at the same dose of 47.5 dpa. By using preconditioned samples, this research focuses on the ability to replicate the growth of microstructural features with heavy ion irradiation that have already been nucleated. Dislocation loops, cavities, precipitates, and radiation induced segregation were examined.

This material is based upon work supported under an Integrated University Program Graduate Fellowship. In addition, this work is supported by the U.S. Department of Energy Nuclear Energy University Program (NEUP) and Nuclear Science User Facilities (NSUF) under grant DE-NE0008520.



A visual comparison of faulted dislocation loops observed with TEM rel-rod imaging in neutron (N) and neutron + ion ((N) + (I)) irradiated samples where ion irradiations were conducted at 380°C, 1x10⁻³ dpa/s.



Measured faulted loop dislocation density and average diameter in neutron (N) and neutron + ion ((N) + (I)) irradiated samples where ion irradiations were conducted at 380°C, 1x10⁻³ dpa/s.

EXPLORATION OF PLANAR DIFFUSION COUPLES WITH REPRESENTATIVE TRISO PYC/SiC MICROSTRUCTURE FOR IRRADIATION TESTING

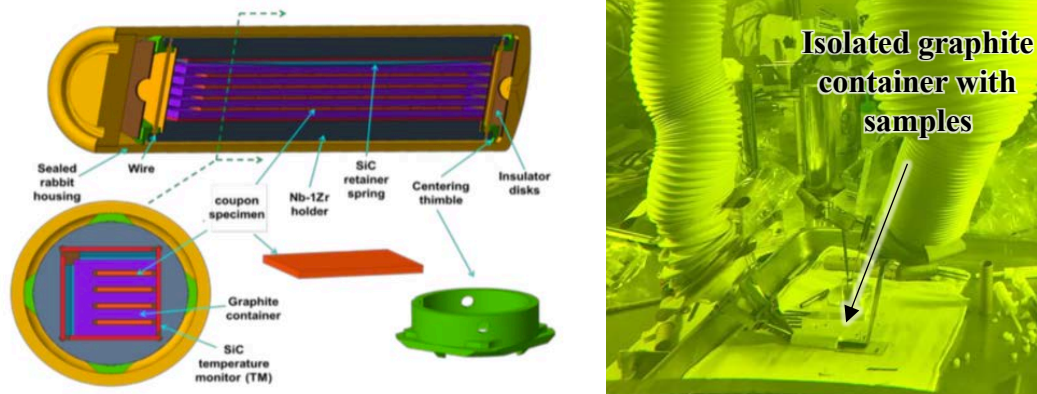
T.J. Gerczak¹, F. Naab², O. Toader²

¹Nuclear Fuel Materials Group, Oak Ridge National Laboratory

²Department of Nuclear Engineering and Radiological Sciences, University of Michigan

Release of fission products from intact tri-structural isotropic (TRISO) coated particle fuel contributes to the source term and limits the operational lifetime of the fuel. In the TRISO fuel design, the silicon carbide (SiC) layer is the primary barrier for release of metallic fission products not retained in the kernel. Release from intact particles is assumed to be dictated by diffusive transport across the SiC barrier layer and is likely impacted by the SiC microstructure and nature of the inner pyrolytic carbon (IPyC) layer. Planar diffusion couples have been fabricated to study diffusion of relevant fission product systems (Ag, Ag+Pd, Eu, and Sr) in representative TRISO materials produced via fluidized-bed chemical vapor deposition. The diffusion couples explore the impact of SiC grain size and PyC density on diffusion. Both diffusion in-reactor and thermal diffusion are being explored. The PyC and SiC diffusion couple layers were deposited on a planar substrate at Oak Ridge National Laboratory (ORNL). The planar geometry facilitates depth profiling relative to the spherical TRISO particle geometry. The fission product species were introduced to the PyC via direct ion implantation using the 400 kV implanter at the Michigan Ion Beam Laboratory through the Department of Energy Nation Science User Facility (NSUF) access. The total flux was controlled to mimic the fission product concentration in TRISO particles at end-of-life. The implantation approach was vital to facilitating diffusion couple SiC-seal-coating to produce an isolated system which facilitates neutron irradiation and high temperature thermal exposures. A total of 120 diffusion couples have been successfully produced and 60 have been irradiated in the High Flux Isotope Reactor at ORNL to 1 and 2 dpa at ~1150°C. Samples are awaiting characterization to determine the potential for radiation enhanced diffusion in the TRISO fuel materials system.

This research is being performed using funding received from the DOE Office of Nuclear Energy's Nuclear Energy University Program through a joint NEET/NEUP R&D with NSUF access award (Project 16-10764).



(Left) schematic of HFIR irradiation capsule with sample (“coupon specimen”)[1] and (right) disassembly of irradiation capsule in the Irradiated Materials Examination and Testing facility.

RADIATION TOLERANCE OF ADDITIVELY MANUFACTURED HT-9 FERRITIC/MARTENSITIC STEEL FOR NUCLEAR POWER APPLICATIONS

K.G. Field¹, S. Taller², N. Sridharan¹

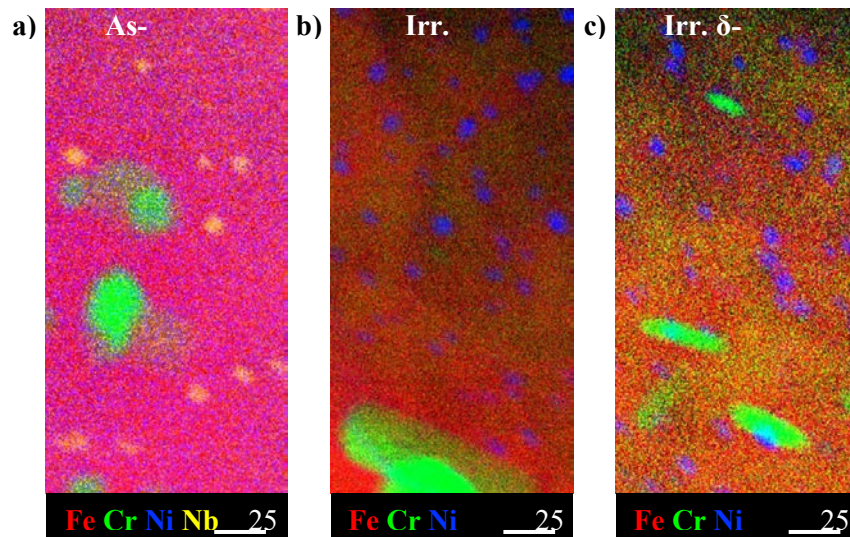
¹Oak Ridge National Laboratory, Oak Ridge, TN

²Department of Nuclear Engineering and Radiological Sciences, University of Michigan

Ferritic martensitic (FM) steels are candidate materials for high-dose applications in advanced nuclear reactor power applications due to their low swelling rates. FM steels are known to degrade in these high dose applications due to irradiation hardening, helium embrittlement, and swelling. The use of additive manufacturing, including directed energy deposition (DED) techniques, is gaining increasing acceptance for consideration in the production of commercial nuclear reactor components. However, parallels with, or tangent to, the commonly identified degradation modes in FM steels have yet to be demonstrated for DED material. Here, a FM steel, HT-9, was produced using powder-blown laser DED at Oak Ridge National Laboratory's Manufacturing Demonstration Facility (MDF) and then irradiated at the Michigan Ion Beam Laboratory (MIBL) to a total damage dose of 50 displacements per atom (dpa) at 460°C using Fe⁺⁺ ions to rapidly assess the radiation tolerance of HT-9 DED material.

The figure below shows the preliminary results of as-received and irradiated HT-9 DED material using scanning transmission electron microscopy coupled with energy dispersive X-ray spectroscopy (STEM/EDS) spectrum imaging. In the as-received condition (a) the martensitic laths contain a dispersion of M₂₃C₆ carbides (green contrast in image) and Nb-rich MX (yellow contrast in image) precipitates. After irradiation, the M₂₃C₆ carbides are still present in the microstructure while the Nb-rich MX precipitates are no longer present suggesting MX instability under high dose, high dose rate irradiations. The STEM/EDS does reveal the formation of Ni-Si rich clusters to form after irradiation in both the martensite laths (b) and the δ-Ferrite grains (c) – blue contrast in figure. In addition, suspected M₂X precipitates are found in the irradiated δ-Ferrite grains. These initial findings are consistent with recent results generated at MIBL on conventionally processed HT-9 alloys irradiated to similar conditions.

This work was supported by the U.S. Department of Energy, Office of Nuclear Energy under DOE Idaho Operations Office Contract DE-AC07-051D14517 as part of a Nuclear Science User Facilities experiment.



Spectrum image maps showing precipitate distributions in additively manufactured HT-9 in a) the as-received condition (martensite), b) the ion irradiated condition (martensite) and c) the ion irradiated condition (ferrite).

HE⁺⁺ IRRADIATION OF AEROSOL JET PRINTED CU, AG AND NI STRUCTURES

K. Fujimoto¹, T. Unruh², A. Fujimoto¹, D. Estrada¹, M. McMurtrey², O. Toader³ and G.S. Was³

¹Micron School of Materials Science and Engineering, Boise State University

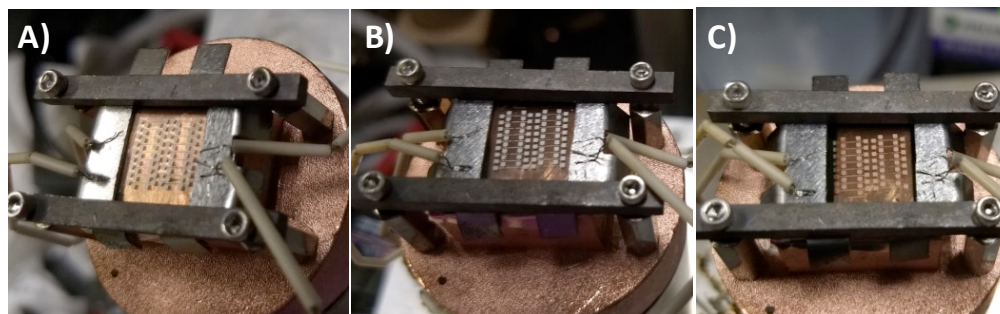
²Idaho National Laboratory

³Department of Nuclear Engineering and Radiological Sciences, University of Michigan

This study aims to examine the effects of He⁺⁺ irradiation on aerosol jet printed (AJP) Ag, Cu and Ni structures to begin to define a library of materials for advanced manufacturing (AM) within the nuclear industry. Establishing this library will require the investigation of several families of electronic materials including metals, semiconductors, and insulators. For this preliminary study, a graded approach is employed to rapidly down select the materials library for advanced manufacturing of in-pile sensors by irradiating AJP structures so that a comparison of their properties can be made against bulk properties. Irradiated materials were four-point structures printed on sapphire substrates utilizing commercially available Ag, Ni and Cu nanoparticle inks with an Optomec Aerosol Jet 200 system. Samples were prepared at Boise State University and began with a pre-processing of sapphire substrates to include O₂ plasma etch at 100 W for 60 sec, followed by sputtering of a 5 nm Ti layer. The Ti layer was then oxidized to form a non-conductive layer to minimize interference with electrical measurements. Post-processing involved sintering of printed structures and the addition of a 300 nm thick chromium layer located along the left and right edges of the sample. The chromium layer was isolated from the printed devices and was used to ground the sample to the sample stage. Resistance measurements were obtained both pre and post-irradiation with preliminary results exhibiting a decrease in resistance for each material for all three doses.

To investigate the irradiation response to He⁺⁺ a total of seventeen irradiation experiments were performed using the 1.7 MV Maize Tandatron accelerator to achieve 0.01, 0.05 and 0.25 displacements per atom (dpa) with a beam energy of 3.5 MeV and a stage temperature of 350 °C. A total of nine silver samples having 18 devices each were fabricated, and sets of three samples were annealed at 500 °C, 600 °C or 700 °C for 30 min. Three nickel samples containing 18 devices each were sintered at 800 °C for 30 minutes, and two sets of three nickel samples each containing 18 devices were sintered at 800°C. Five copper samples were fabricated with a set of three being sintered at 500 °C and a set of two at 600 °C. He⁺⁺ fluence varied per irradiation experiment and irradiation time was adjusted to achieve the desired dpa. The beam energy was chosen to ensure that He⁺⁺ ions fully penetrated the printed structures while achieving the desired dpa. Temperature control was made with thermocouples attached to a plate making connection with the chromium layer of the sample. The sample setup is shown in Figs. a-c. Thermocouple measurements were used to calibrate the thermal imager to ensure that uniform heating of the irradiated area. Additionally, pressure, temperature, fluence and beam currents were recorded during irradiation experiments.

This work was supported through the Department of Energy In-Pile Instrumentation program, under DOE Idaho Operations Office Contract DE-AC07-05ID14517. We'd also like to acknowledge infrastructure support through the DOE NSUF under award #DE-NE0008677.



Sample irradiation stage with (A) silver, (B) nickel and (C) copper AJP four-point structures on sapphire.

Non-NSUF Projects

RADIATION EFFECTS IN FIELD-EFFECT TRANSISTORS BASED ON ATOMICALLY-THIN MoS₂

A. Arnold¹, T. Shi², I. Jovanovic², S. Das³

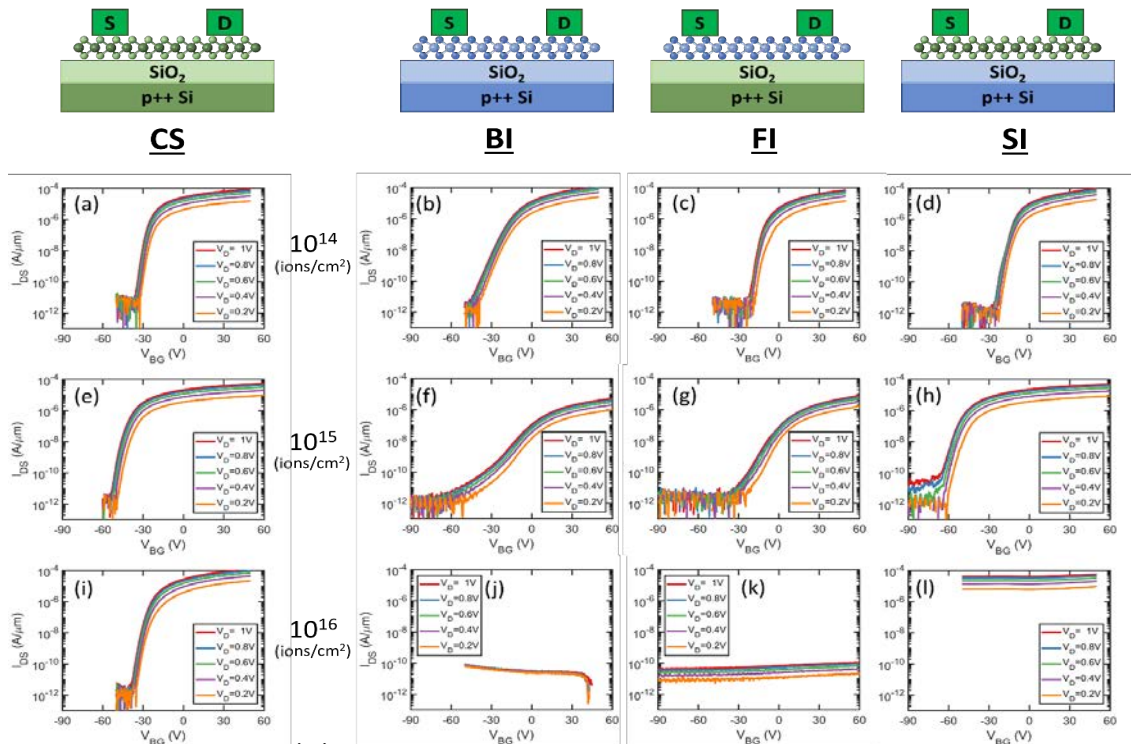
¹Electrical Engineering, Pennsylvania State University

²Department of Nuclear Engineering and Radiological Sciences

³Engineering Science and Mechanics, Pennsylvania State University

Understanding the radiation resilience of transistors based upon ultrathin (two-dimensional) channel materials is important for their use in high-radiation environment such as space. The impact of ion irradiation on the electric behavior of MoS₂-based field-effect transistors (FET) was studied using He⁺ beam and p⁺ beam at different fluences. A new approach was adopted to decouple the different damage effects by partially irradiating the different transistor components. Three groups of samples were investigated: devices with only substrate irradiated (SI); devices with only MoS₂ flake irradiated (FI), and devices with both substrate and MoS₂ flake irradiated (BI). With this new approach, we were able to correlate the change in FET I-V characteristics to the damage in the substrate and MoS₂ channel layer respectively. The impact on device mobility, subthreshold slope and threshold voltage were also measured. We found that ultrathin MoS₂ nanosheets can easily withstand proton and helium irradiation with fluences as high as $\sim 10^{16}$ ions/cm² and $\sim 10^{15}$ ions/cm², respectively, corresponding to hundreds to thousands of years of exposure to radiation in space.

The work of A. J. A. and S. D. was supported by Grant Number FA9550-17-1-0018 from Air Force Office of Scientific Research (AFOSR) through the Young Investigator Program.



Representative transfer characteristics of MoS₂ FETs from unirradiated control sample (CS) with neither the flakes nor the substrate being irradiated and post radiation samples BI, FI and SI. 390 keV He⁺ ions were used at a total fluence of a-d) 10¹⁴ He ions/cm², e-h) 10¹⁵ He ions/cm², and i-l) 10¹⁶ He ions/cm².

RAPID SIMULATION OF VOID SWELLING IN PWR INTERNALS

M. Song¹, K.G. Field², C. Topbasi³, J.T. Busby², G.S. Was¹

¹Nuclear Engineering and Radiological Sciences, University of Michigan

²Materials Science and Technology Division, Oak Ridge National Laboratory, Oak Ridge, TN

³Electric Power Research Institute, Palo Alto, CA

Most nuclear reactors in the United States and other countries are expected to continue operation beyond their original operating licenses to as many as 80 or even 100 years. Pressurized water reactor (PWR) internals are expected to experience high damage doses that can exceed 100 dpa by the end of the second license renewal, therefore, there is a need for data and validated models to predict the degree of irradiation damage expected in austenitic stainless steel internals. Materials test reactor irradiation is impractical because the rate of damage accumulation is comparable to that in commercial reactors. The only practical means of obtaining irradiated microstructures at high damage dose in a short amount of time and at modest cost is ion irradiation. Proton irradiation has proven to be extremely useful in emulating the radiation damage microstructure in stainless steels under light water reactor temperatures and up to modest (~10 dpa) damage levels. However, access to the highest damage regimes (e.g. >100 dpa) requires the use of self-ion irradiation. The goal of this project is to use self-ion (Ni^{3+}) irradiation to capture the growth processes at higher damage levels of cold-worked 316L SS after the pre-cursor nucleation processes are completed via irradiation in reactor.

Thin disks 3 mm in diameter and 0.2 mm thick were cut from flux thimble tubes with various neutron damage levels 0, 38-41, 72-75, and 100 dpa. Two irradiation experiments were performed on 0 dpa samples using 9 MeV Ni^{3+} ions from Wolverine at temperatures of 390 and 410°C to a damage level of 38 dpa. The experimental temperature was selected based on Mansur's invariance theory to compensate for the dose rate difference between neutron irradiation condition (~320°C and $5.5\text{-}13.5 \times 10^{-8}$ dpa/s) and the dose rate of 8×10^{-4} dpa/s used in the ion irradiation. Microstructure was evaluated at a depth of 800 nm below the surface as shown in Figure (a). The depth was selected based on minimal microstructural impacts from both free surface and injected interstitials. Temperature control was achieved using thermocouples, spot-welded to dummy samples of same materials, thickness, and configuration that were not irradiated. The temperature of irradiated samples was monitored during the entire irradiation with a thermal camera, which was pre-calibrated against the four thermal couples at the target temperature without beam. The infrared image from the thermal camera is shown in Figure (b). The temperature histogram is shown in Figure (c). A high degree of temperature control was achieved as the value of 2σ was 1.7°C about an average temperature of 391.7°C. The microstructure of the ion-irradiated samples will be analyzed and compared to that of neutron irradiated samples at the same dose to determine the temperature that best captures all of the radiation induced microstructural features.

This work was supported by the Electric Power Research Institute under contract number 10002154 and 10002164.



Displacement rate and implantation ion curves for 9 MeV Ni^{3+} in 316L SS (a), infrared image of irradiation stage with thin disk samples (b), and temperature histogram of the ion irradiation (c)

SCC IN Fe- AND Ni-BASE WELDMENTS FOR LWR SUSTAINABILITY

B.J. Heuser¹, X. Bai², B. Spencer³, G.S. Was⁴

¹Department of Nuclear, Plasma, and Radiological Engineering, University of Illinois

²Department of Materials Science and Engineering, Virginia Tech

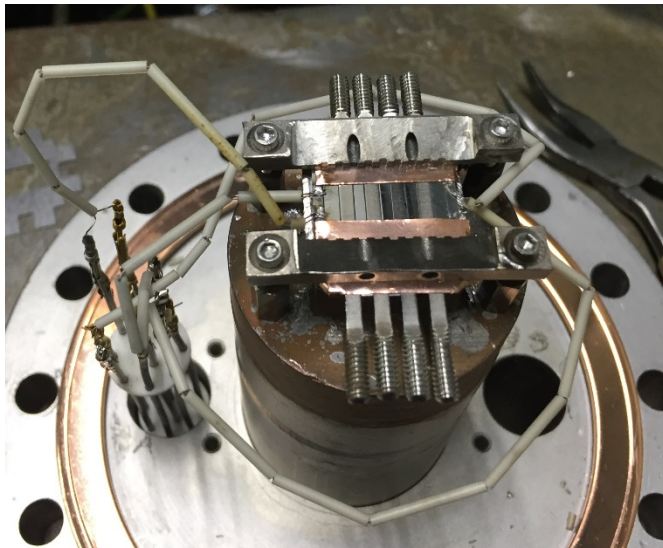
³Fuels Modeling & Simulation, Idaho National Laboratory

⁴Department of Nuclear Engineering and Radiological Sciences, University of Michigan

The objective of this project is to provide experimental data on the performance of Alloy 308/309 and 82/182 weldments during exposure to environmental factors typical of normal LWR operation in support of the LWRS Program. In particular, the work scope is designed to determine inter-granular stress corrosion cracking (IGSCC) susceptibility with respect to radiation damage and LWR primary coolant chemistry. The goal is to correlate crack initiation and IGSCC to 1) grain boundary orientation, 2) local grain boundary chemistry and oxidation, 3) and localized deformation, and 4) dpa displacement cascade damage. The experimental protocols are designed to separate the effect of irradiation and associated radiation damage from environmental factors such as LWR water chemistry and applied load and to determine the synergistic effect of irradiation, water chemistry, and tensile stress. In addition, modeling activities are proposed that capture salient features of the materials response of these alloys to LWR environments. The combined experimental and computational methodology is anticipated to improve the predictive capability of Grizzly using a novel extended finite element method (XFEM). The proposed project will be supportive of the LWRS Program in two ways. First, it will expand the knowledge base to include the behavior of weldments found in LWRs. Second, it will serve as input into a modeling component to this project, which in turn will lead to enhanced predictive capability of Grizzly.

We have initiated SSR immersion testing of an EPRI 508LAS-304L weldment under different LWR water chemistry conditions using the UIUC recirculating loop autoclave. In addition, the first set of proton irradiation experiments were performed at the MIBL in October of 2018. The figure below shows four tensile specimens and six TEM specimens mounted prior to the irradiation experiment. These specimens were successfully irradiated at 360°C to approximately 3 dpa (quick K-P model calculation via TRIM). The tensile specimens will undergo subsequent SSR immersion testing. The TEM specimens will undergo immersion testing. Additional proton irradiations are planned.

This work was supported by the U.S. Department of Energy, Nuclear Energy University Programs under contract DE-NE0008699.



Mounted tensile and TEM specimens prior to proton irradiation at 360°C to approximately 3 dpa.

ACCELERATED CORROSION IN ION IRRADIATED *CuCrZr* ALLOYS TO SIMULATE DIVERTOR COOLANT PIPE CONDITIONS

J. J. H. Lim¹, G. Fulton¹, R. Hanbury², G.S. Was²

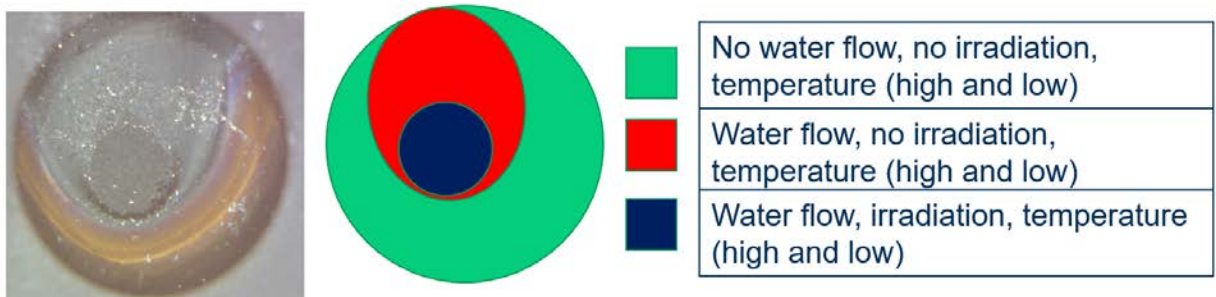
¹United Kingdom Atomic Energy Authority, UK

²Department of Nuclear Engineering and Radiological Sciences, University of Michigan

The goal of this study is to investigate the simultaneous effect of displacement damage and radiolysis on the corrosion of *ITER* grade *CuCrZr* coolant pipes in the divertor. To present, lifetime predictions of *CuCrZr* coolant pipes have been based on mechanical arguments [1]–[3] and only limited oxidation on *CuCrZr* components has been observed by mimicking the oxidizing radiolysis products with additions of hydrogen peroxide and dissolved oxygen [4]–[6]. These studies neglect the effect of displacement damage on the kinetics of oxide growth. This study aims to determine whether simultaneous displacement damage dictates the effective component lifetime for *ITER* grade divertor coolant pipes.

To investigate the effects of simultaneous displacement damage and radiolysis on the corrosion of *CuCrZr*, the irradiation accelerated corrosion (*IAC*) facility at Michigan Ion Beam Laboratory (*MIBL*) was used [7]. This facility couples a high pressure sealed autoclave on the end of a beamline. Two 24 – 26 μm ultra-thin 8mm diameter *CuCrZr* disks were polished on both sides with colloidal silica and irradiated for 48 h using the Wolverine accelerator ($5.43\text{MeV } H^+$, $5.03 \times 10^9 \text{s}^{-1}\text{mm}^{-2}$) at 325°C and 35°C , to a total dose of 0.31 – 0.32 *dpa*. These temperatures correspond to the upper estimate for water coolant temperatures in fusion reactors and ambient beam heating conditions. Neutral pH, de-ionized ($< 200\text{ppb } O_2$) water was used during the irradiation. Diagnostic measurements of temperature, dissolved oxygen content, beam current and chamber pressure were recorded during the irradiation. Preliminary results indicate that displacement damage has a direct impact on corrosion kinetics as shown in the figure.

This work has been supported by the RCUK Energy Programme [grant number EP/P012450/1] and has been carried out within the framework of the EUROfusion Consortium, receiving funding from the Euratom research and training program 2014-2018 under grant agreement No 633053. The views and opinions expressed therein do not necessarily reflect those of the European Commission. The research also used UKAEA’s Materials Research Facility, which has been funded by and is part of the UK’s National Nuclear User Facility and Henry Royce Institute for Advanced Materials (EP/P021727/1).



Oxidation behavior observed in *CuCrZr* at 325°C tested in the Irradiation Accelerated Corrosion beam line at *MIBL* (total dose 0.31 – 0.32 *dpa*) showing increased oxidation rate under irradiation areas (blue)

DETERMINATION OF HELIUM CONTENT WITH THIN FOIL ENERGY DEGRADATION USING ELASTIC BACKSCATTERING SPECTROMETRY

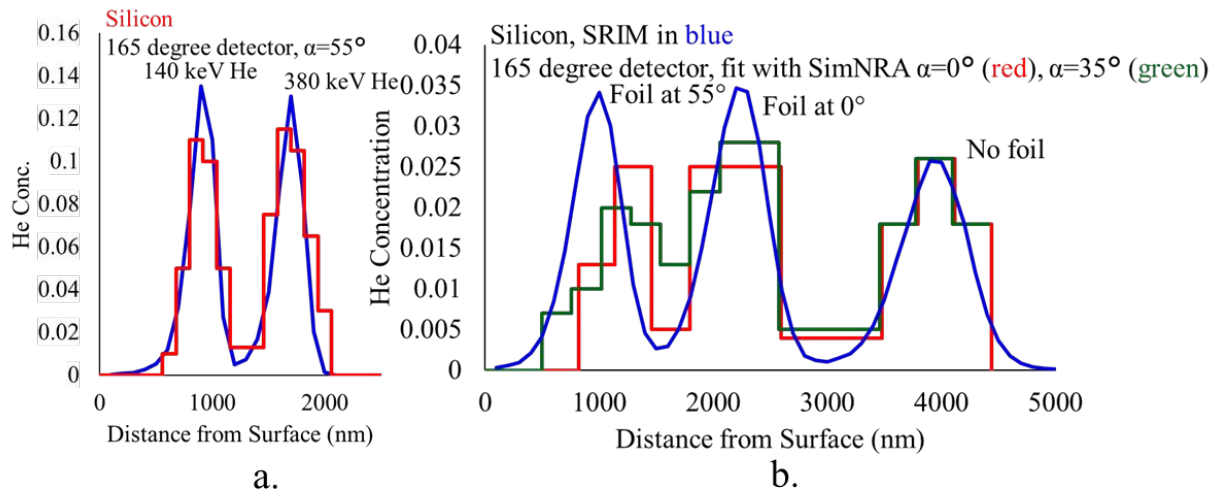
S. Taller, F. Naab, D. Woodley, G. S. Was

Department of Nuclear Engineering and Radiological Sciences, University of Michigan

The effects of helium and hydrogen must be included in ion irradiation experiments to emulate the production of these gases by transmutation in reactor. In previous years, a calculation methodology using the Stopping and Range of Ions in Matter (SRIM) program suite was developed to quantify the spatial distribution, implantation depth and amount of energy-degraded and implanted light ions when using a thin foil rotating energy degrader during multi-ion beam irradiation. Previous benchmarks used deuterium ions to benchmark the implanted fluence and profile by comparing the calculation methodology with secondary ion mass spectrometry. However, the relatively large mass difference between deuterium and helium leads to uncertainty when extrapolating outside the benchmarked conditions. Therefore, a new benchmark using helium is required to confirm the calculation methodology.

Elastic backscattering spectrometry (EBS) was used to profile the helium concentration as a function of distance from the surface. To validate the technique, samples of silicon and T91 heat C2269 were implanted with 140 keV helium ions and 380 keV helium ions sequentially to fluences of 2×10^{17} ions/cm² for each energy. The location of the implanted helium profiles agreed well with calculations using SRIM in both height and total fluence providing confidence in the ion beam analysis measurement technique. To assess the foil degrader methodology, sequential 2.1 MeV helium implantations were performed in silicon without the thin foil energy degrader, with the foil degrader held perpendicular to the ion beam (0° of rotation) and with the foil rotated to a high angle relative to the ion beam (55° of rotation). The total helium fluence implanted for each condition was excellent between the calculation methodology and measured fluence from EBS with the location of the helium distribution also in good agreement. These results provided a benchmark to confirm the accuracy of the helium foil degrader methodology used at the Michigan Ion Beam Laboratory.

This work is supported by the U.S. Department of Energy, Office of Nuclear Energy.



Helium concentration profiles for a) silicon implanted with 140 keV helium ions and 380 keV helium ions sequentially to fluences of 2×10^{17} ions/cm² for each energy with SRIM in blue and EBS in red, and b) silicon implanted with 2.1 MeV He²⁺ without a foil degrader, with the foil degrader at 0° and at 55°.

HIGH FIDELITY ION BEAM SIMULATION OF HIGH DOSE NEUTRON IRRADIATION

S. Taller¹, Z. Jiao¹, K. G. Field², G.S. Was¹

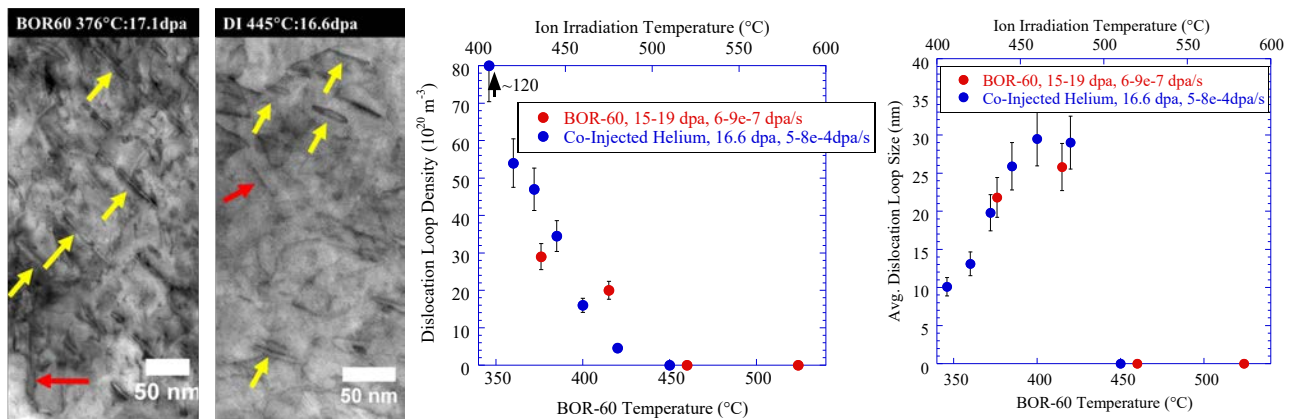
¹Department of Nuclear Engineering and Radiological Sciences, University of Michigan

²Materials Science and Technology Division, Oak Ridge National Laboratory

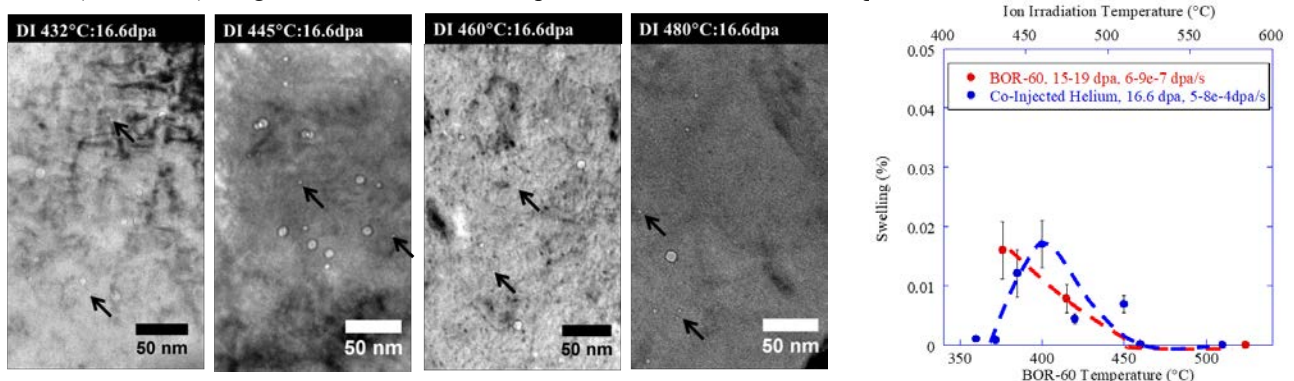
Traditional research efforts to understand radiation-induced processes in materials require years of comprehensive post-irradiation characterization effort of test reactor produced neutron irradiated material. The same levels of radiation damage can be achieved using heavy ion irradiation under tightly controlled conditions in days or weeks instead of years in a nuclear reactor, albeit with several challenges. The purpose of this work is to address these challenges in using ion irradiation as a surrogate for neutron irradiation.

Several dual ion irradiations were performed using 5.0 MeV defocused Fe⁺⁺ ions to damage the material while simultaneously injecting He⁺⁺ ions in a fixed ratio to emulate gas buildup from nuclear transmutation reactions. Bars of T91 were dual ion irradiated up to 35 dpa with 4 appm helium per dpa from 420°C to 570°C to compare with multiple conditions from the BOR-60 fast reactor to the same level of damage and examine the role of temperature on the irradiated microstructure. These specimens are being examined with transmission electron microscopy and atom probe tomography to determine the effects of simultaneous helium injection and radiation damage on the irradiated microstructure of these materials.

This work is supported by the U.S. Department of Energy under award DE-NE0000639.



A comparison of STEM Bright Field (BF) images in T91 30176 irradiated with neutrons in BOR-60 or dual ions at MIBL (left) under [100] or [110] zone axis conditions to distinguish between a<100> (yellow arrows) and a/2<111> (red arrows) Burgers vector dislocation loops to determine dislocation loop density and average diameter.



Cavities were imaged in STEM BF and High Angle Annular Dark Field (HAADF). Cavities examined up to 1000 nm from the free surface of ion-irradiated T91 in 100 nm increments to quantify the amount of swelling. Underfocused TEM BF images are shown here for clarity of cavity observation with small bubbles highlighted with arrows. Cavities are visible as white spots with a darker fringe around it.

EFFECT ON IRRADIATION ON THE CORROSION OF 316L STAINLESS STEEL

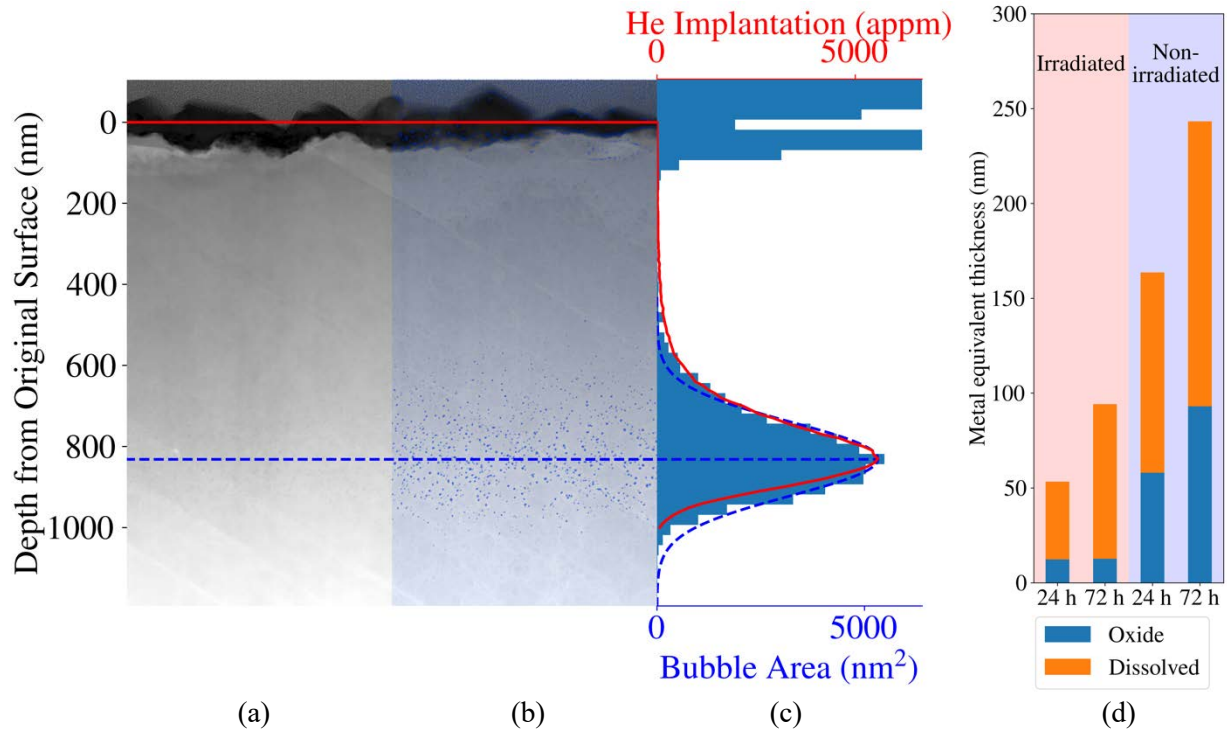
R.D. Hanbury, G.S. Was

Department of Nuclear Engineering and Radiological Sciences, University of Michigan

Three *in situ* proton irradiation corrosion exposures of 316L heat 626032 were completed and characterized this year using the Wolverine 3 MV tandem accelerator on beamline 3. All experiments shared the following exposure conditions: 5.4 MeV raster-scanned H⁺ beam, 7×10^{-7} dpa/s, ~ 700 kGy/s, 320°C, 13.1 MPa, in 3 wppm H₂ water. Samples were mounted with a precipitation hardened steel (17-4 PH) backing disc to minimize deformation and residual radioactivity on the sample material. Two samples were hot-implanted with helium at 550°C to 10^{16} He/cm² before exposure to produce a bubble marker layer for measuring oxide dissolution after exposure for 24 and 72 hours. The third sample had a surface parallel to the beam immersed in the autoclave for 24 hours to isolate the effect of radiolysis on corrosion from displacement damage.

Results from the helium implanted experiments show that radiation suppresses the total oxidation in all radiation affected regions relative to non-irradiated oxides. The radiolysis isolation experiment showed a marked decrease in the oxide film thickness in areas directly and indirectly exposed to the proton beam. Together, these results indicate that radiolysis is the driving force for reducing the total corrosion rate under irradiation.

This research is supported by EDF contract number 8610-5920005571 and the Rickover Fellowship Program.



HAADF STEM micrograph of bubble marker layer (a) under oxide formed under direct irradiation, (b) overlaid with a probability map from Weka segmentation, and (c) histogram of bubble density used to back-calculate the original metal surface. The oxide thickness and dissolution measurements are plotted (d) for 24 and 72 hours in both irradiated and non-irradiated cases.

IRRADIATION EFFECTS IN FERRITIC-MARTENSITIC STEELS AT VERY HIGH DAMAGE LEVELS

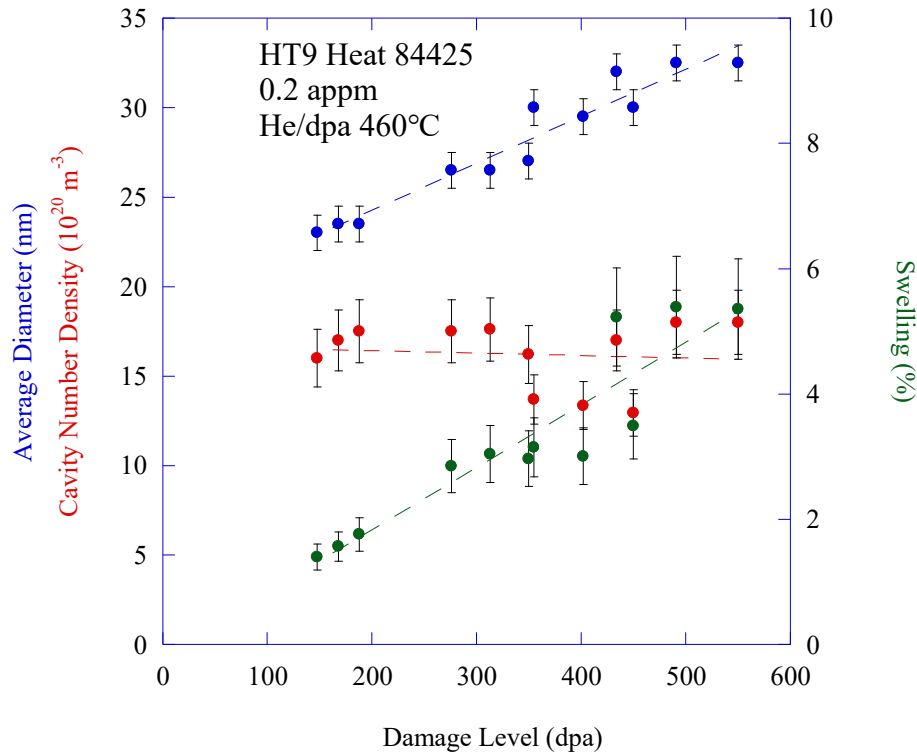
D. Woodley, Z. Jiao, K. Sun, G.S. Was

Department of Nuclear Engineering and Radiological Sciences, University of Michigan

Understanding the microstructural evolution in ferritic-martensitic steels is important for predicting the safety and reliability of future reactors. Dual ion irradiation experiments have been performed on heat 84425 of HT9, a ferritic-martensitic steel, to examine the effects of increased damage level on bubbles and cavities. Irradiations were performed at the Michigan Ion Beam Laboratory with 5 MeV Fe^{++} ions from a 3 MV Pelletron accelerator and 2.05-2.18 MeV He^{++} ions, degraded by a rotating aluminum foil, from a 1.7 MeV Tandemtron accelerator to simulate damage and transmutation gas, respectively. Experiments were performed to 188, 350, 450 and 550 dpa at 460°C with a constant helium-to-dpa ratio of 4 appm He/dpa. The microstructural behavior was examined using both conventional transmission electron microscopy and scanning transmission electron microscopy. The bubble and cavity behavior were examined for each condition to map out the effect of increased damage level on swelling.

A bimodal size distribution was observed at all damage levels indicating the presence of both bubbles and cavities. The average cavity diameter increased with increasing damage level while the number density was constant. The increasing diameter and constant density led to increasing swelling with increasing damage level. The maximum swelling attained was 5.3% at 550 dpa.

This work is supported by the TerraPower, LLC.



Cavity diameter and density in HT9 heat 84425 as a function of damage level at 460°C with a helium-to-dpa ratio of 4 appm He/dpa. The plot ignores the bubbles and smaller cavities (diameter <10 nm) for all cases. The lines are there to guide the eye and do not represent trend lines.

LOCALIZED DEFORMATION AND INTERGRANULAR FRACTURE OF IRRADIATED ALLOYS UNDER EXTREME ENVIRONMENTAL CONDITIONS

D.C. Johnson¹, G.S. Was¹, B. Kuhr², D. Farkas², R. Mo³, I.M. Robertson³

¹Department of Nuclear Engineering and Radiological Sciences, University of Michigan

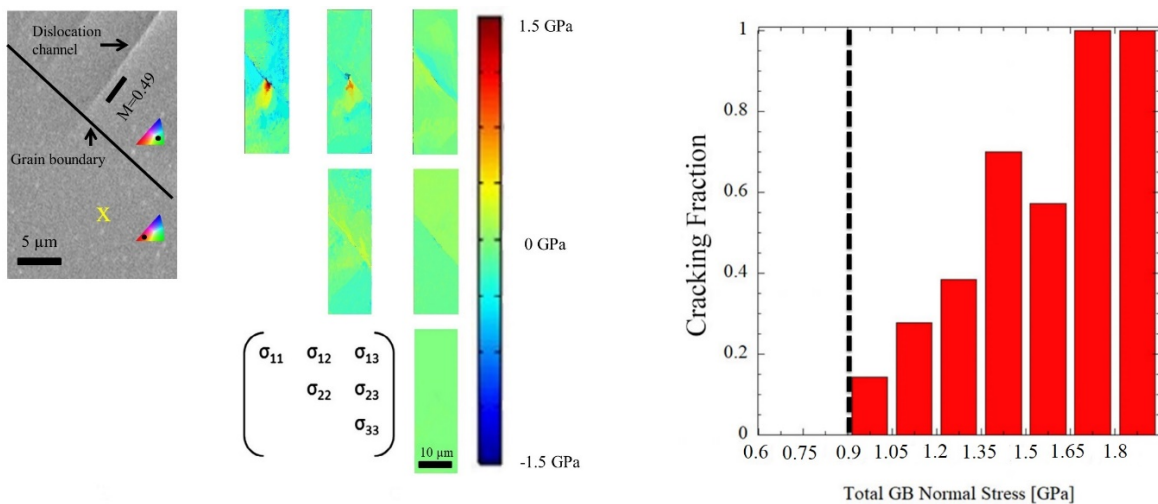
²Department of Materials Science and Engineering, Virginia Tech University

³Department of Materials Science and Engineering, University of Wisconsin

The goal of this project is to determine the role of localized deformation in austenitic steel during irradiation assisted stress corrosion cracking (IASCC). The project is a collaboration between the University of Michigan, University of Wisconsin, and Virginia Tech University with the purpose of obtaining better understanding of the mechanisms involved in IASCC. Samples are being irradiated at the University of Michigan and strained in constant extension rate tensile (CERT) tests to study the cracking behavior. Atomistic models of the experiments are being developed by Dr. Farkas' group at Virginia Tech University, and irradiated samples will be strained in-situ in a TEM by Dr. Robertson's group at the University of Wisconsin.

This year, two irradiations were performed using 2 MeV protons at 360 °C on a 13Cr15Ni lab purity alloy in the Tandem Accelerator located in the Michigan Ion Beam Laboratory. The first irradiation reached a damage level of 5 dpa while the second irradiation went to 0.5 dpa to study the stress state developed at lower damage. Tensile bar samples from these irradiations were used to quantify the stress component normal to grain boundaries at discontinuous dislocation channel – grain boundary interaction sites, and then relate that to cracking. Samples were strained in high temperature argon (288°C) to produce dislocation channels. These channels were either arrested at the grain boundary or transmitted to the adjacent grain. In both cases, residual elastic stress values were calculated using High Resolution Electron Backscatter Diffraction. Once stresses had been characterized, the samples were strained further in water, and cracking behavior was characterized with respect to the known stress levels in the dislocation channel/grain boundary intersections. The cracking behavior of these irradiated samples showed a clear correlation between the stress acting normal to the grain boundary and intergranular fracture susceptibility.

This research has been supported by the Basic Energy Science office of the U.S. Department of Energy under grant DE-FG02-08ER46525.



(a) Stress tensor calculated near a discontinuous channel-GB interaction site, and b) dependence of the cracking susceptibility on the magnitude of the stress acting normal to the grain boundary plane.

ION IRRADIATION OF A Fe-15Cr MODEL ALLOY

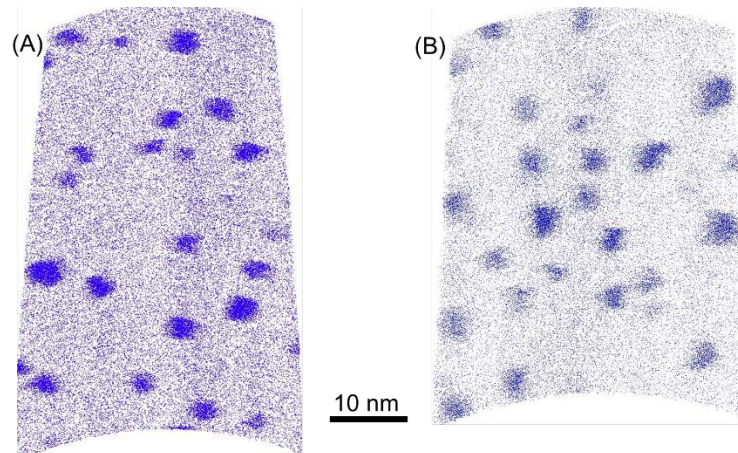
K.N. Thomas, Z. Jiao, G.S. Was

Department of Nuclear Engineering and Radiological Sciences, University of Michigan

High-chromium ferritic-martensitic (F-M) alloys are candidates for future nuclear power plants due to the corrosion resistance and low swelling under irradiation. However, with chromium concentrations above ~9% and at lower temperatures below ~500°C, the F-M alloys are susceptible to the formation of Cr-rich α' precipitates. Research has shown that the α' precipitates can be formed under thermal aging, as well as neutron, electron, and proton irradiation, but there is difficulty in the α' precipitate formation under heavy ion irradiation due to ballistic dissolution.

Model alloy Fe-15Cr was irradiated at the Michigan Ion Beam Laboratory (MIBL) in a series of experiments. The first experiment utilized 2 MeV protons to 1 dpa at 400°C at 1.0×10^{-5} dpa/s. This irradiation established an α' precipitate microstructure within the samples, as characterized using atom probe tomography (APT). Two subsequent irradiations were performed on the proton irradiated samples with 4.4 MeV Fe^{3+} or Fe^{2+} at 300°C at 1.0×10^{-5} dpa/s to 1 dpa, and 1.0×10^{-3} dpa/s to 1 dpa and 3 dpa, respectively. The effects of the heavy ion irradiation on the α' precipitate was observed using APT to determine the effects of the damage rate on the α' precipitates.

This work is supported by the U.S. Department of Energy under award DE-NE0000639.



Representative volume ($70 \times 25 \times 5 \text{ nm}^3$) of α' precipitates in Fe-15Cr displaying 75% Cr atoms (in blue). (A) proton irradiated (2 MeV) to 1 dpa at 1.0×10^{-5} dpa/s at 400°C. (B) proton irradiated (2 MeV) to 1 dpa at 1.0×10^{-5} dpa/s at 400°C followed by heavy ion irradiated (4.4 MeV Fe^{3+}) to 1 dpa at 1.0×10^{-5} dpa/s at 300°C.

MECHANICAL TESTING AND CHARACTERIZATION TO SUPPORT MODERN STRESS CORROSION CRACK INITIATION TESTING ON PROTON-IRRADIATED MATERIAL

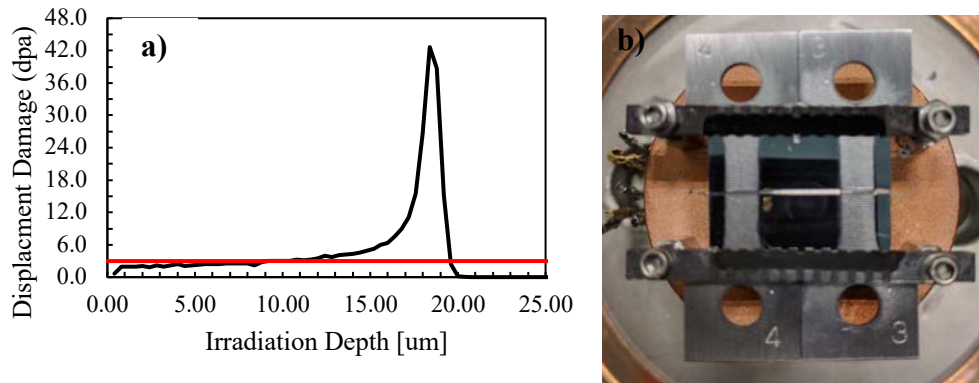
M.A. Mattucci¹, J.M. Smith¹, G.S. Was² and C.D. Judge¹

¹Canadian Nuclear Laboratories (Chalk River Labs), Ontario, Canada

² Department of Nuclear Engineering & Radiological Sciences, University of Michigan

Irradiation assisted stress corrosion cracking (IASCC) is a as complex failure mechanism for which materials exposed to neutron irradiation become more susceptible with increasing fluence and is an active degradation mechanism for stainless steels (SSs) in reactor cores. While proton irradiation has been used to emulate reactor core conditions at a fraction of the time and cost, with reduced activity, it has been limited in applicability partly due to a shallow penetration depth. CNL has developed IASCC initiation testing capabilities for proton irradiated specimens utilizing actively loaded, blunt-notch tensile specimens and in situ crack detection via direct current potential drop (DCPD). The goal is to extend the utility of proton irradiation by employing sensitive DCPD measurements and small volume techniques such as nanoindentation. To this end, Grade 304L SS was irradiated with 3 MeV protons to 3 displacements per atom (dpa) full cascade, using irradiation temperatures of $360\pm 10^\circ\text{C}$ and $100\pm 20^\circ\text{C}$ to emulate neutron irradiation damage in a sink dominated/void swelling regime for two cases: SS in the core of a boiling water reactor or pressurized water reactor ($288\text{-}330^\circ\text{C}$) and SS at the periphery of a CANDU reactor core ($60\text{-}80^\circ\text{C}$).

Post-irradiation defect analysis has been performed using high resolution transmission electron microscopy (TEM) and atom probe tomography (APT) at these two temperature regimes. TEM has been used to characterize the size and density distributions of cavities, loops, and assess radiation induced segregation at grain boundaries. APT is used to characterize cluster formation, and radiation induced segregation. The implications of the microstructure with respect to IASCC susceptibility were studied. Post-irradiation testing involved nanoindentation studies to examine changes in material properties, which support investigations of SCC susceptibility. The characteristic depth for the indentation size effect and the increase in the yield strength from irradiation induced defects were determined and compared to hardening predicted from irradiation defect characterization. Furthermore, the irradiation damage was characterized, as a function of depth from the base of a machined notch and from a polished surface. Spatial distribution of defect accumulation around a blunt flaw were examined in the context of the mechanistic understanding of IASCC.



a) Displacements per atom as a function of irradiation depth for 2MeV protons impinging on 304L SS and b) notched 304L SS tensile samples irradiated at $360\pm 10^\circ\text{C}$.

IRRADIATION ASSISTED STRESS CORROSION CRACKING OF LASER ADDITIVELY MANUFACTURED 316L STAINLESS STEEL

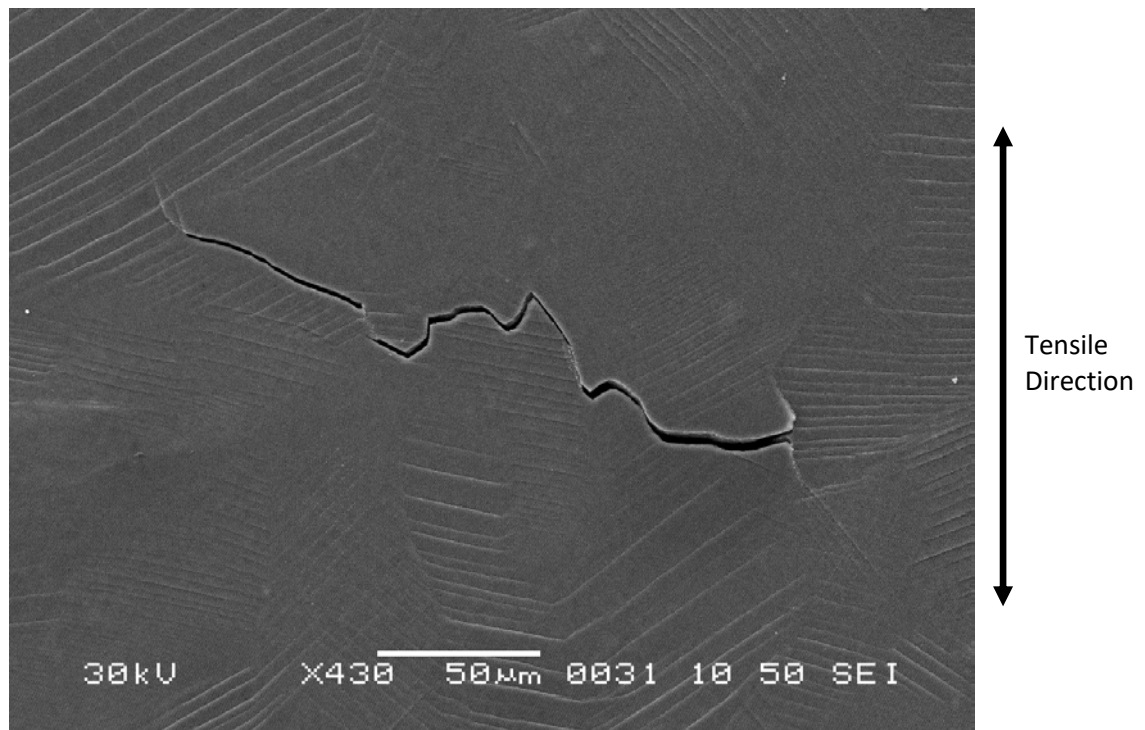
R.D. Hanbury, G.S. Was

Department of Nuclear Engineering and Radiological Sciences, University of Michigan

Wrought and laser additively manufactured (LAM) 316 material was received as tensile bars and TEM (spacer) bars for proton irradiation and subsequent autoclave straining. Material was split into two groups, each containing one tensile bar and one TEM bar of wrought 316 and three tensile bars and three TEM bars of each orientation of the LAM 316 material. Irradiations at 360°C and 2.0 MeV protons were performed on each batch to 1 and 5 dpa. Constant extension rate testing (CERT) was performed on each batch under simulated BWR NWC conditions to 4% plastic strain at a strain rate of $3 \times 10^{-7} \text{ s}^{-1}$.

Both CERT experiments showed similar mechanical behavior between all three orientations of the LAM material. The yield stress for the wrought material was consistently lower than the LAM material, and the wrought bars appeared to have more strain hardening than the LAM did. After straining, four LAM bars were examined in a JEOL SEM for any significant cracking: three 5 dpa bars and one 1 dpa bar. Only the 5 dpa bar parallel to the printing direction exhibited significant cracking; no cracks were observed on any bar from the printing plane or at 1 dpa.

This research is supported by Idaho National Laboratory.



SEM micrograph of intergranular cracking and dislocation channels on a laser additively manufactured 316L stainless steel tensile bar proton irradiated to 5 dpa and constant rate extension tested to 4% strain under simulated BWR NWC conditions.

OXIDATION OF FE-CR-AL ALLOYS IN SIMULATED LWR ENVIRONMENTS DURING IN-SITU PROTON IRRADIATION-CORROSION TESTS

P. Wang¹, D. Bartels², G. S. Was¹

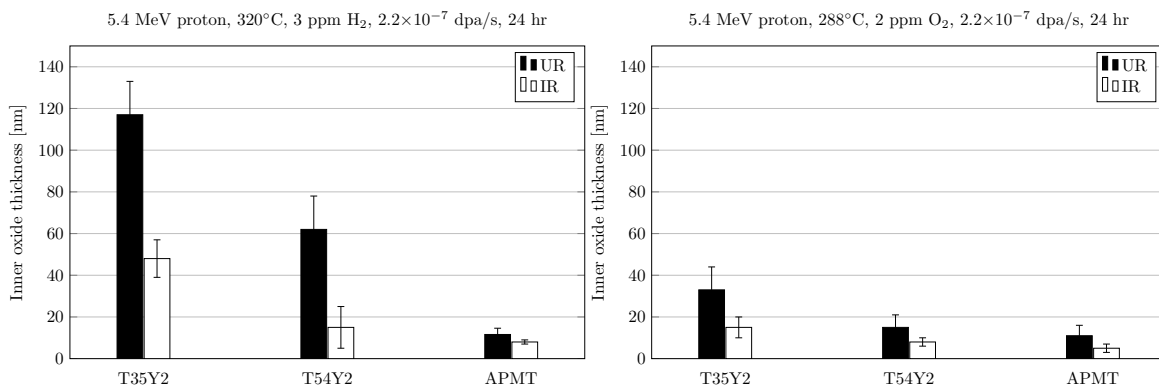
¹Department of Nuclear Engineering and Radiological Sciences, University of Michigan

²Department of Chemistry and Biochemistry, University of Notre Dame

The development of accident tolerant fuels (ATF) is aimed at avoiding the situation that occurred at Fukushima in 2011 where rapid oxidation of Zircaloy cladding resulted in a highly exothermic zirconium-steam reaction, resulted in production of hydrogen, which later combusted and caused damage to the secondary containment. To avoid such occurrences in light water reactors (LWRs), the ATF program was initiated to focus on the replacement of zirconium-based alloys with materials that exhibit slower steam oxidation kinetics. The objective of this work is to assess the corrosion behavior of ATF candidate iron-based alloys under normal LWR operating conditions consisting of high temperature, relevant water chemistry and irradiation.

This research project has focused on several iron-chromium-aluminum (FeCrAl) alloys.: APMT, MA956, and two experimental FeCrAl experimental alloys. For comparison, T91 was studied for which some data exists on the corrosion behavior in water in the range 300-600°C. Experiments were conducted in both PWR primary water at 320°C and BWR normal water chemistry at 288°C, spanning a large range in electrochemical corrosion potential (ECP). Samples were exposed to proton irradiation and corrosive environment simultaneously to assess the roles of displacement damage and environment on corrosion rate. The dose rates to the water in these experiments were very high relative to typical reactor conditions in order to quickly assess whether the alloys might be too radiation-sensitive for reactor service. Extensive post-test characterization has been performed to determine the oxide thickness phases, phase morphologies and composition using a variety of techniques. In general, we found that under reducing conditions (PWR hydrogenated water), the FeCrAl alloys forms a double layered oxide structure, which are very stable, and there should be no problem with using them. In oxidizing conditions there are some tendencies for the inner protective oxide to dissolve away, such conditions may be found at the top-of-core in boiling water reactors, and FeCrAl cladding designs will require careful assessment of whether the alloys are acceptable in that situation.

This research was supported by the DOE-NEUP, Contract No. DE-NE0008272.



Comparison of inner oxide thickness of the ATF candidate alloys after in-situ proton irradiation-corrosion tests in hydrogenated water and normal water chemistry.

ASSESSMENT OF COATINGS TO MITIGATE SHADOW CORROSION USING IN-SITU PROTON IRRADIATION-CORROSION TESTS

P. Wang¹, G. S. Was¹, K. Nowotka²

¹Department of Nuclear Engineering and Radiological Sciences, University of Michigan

²Framatome Germany

Shadow corrosion, as a type of irradiation-assisted galvanic corrosion between dissimilar metals, the shape of the component is often reproduced in the shape of an area of enhanced corrosion, suggestive of shadow cast by the component on the zirconium alloy surface. Shadow corrosion is also closely related to the channel bowing phenomenon, which resulted in control blade interference due to channel distortion.

Several mechanisms have been proposed to explain the appearance of shadow corrosion, and the majority are related to the electrochemical nature of the Zircalloys. However, to date, shadow corrosion has only been observed on samples exposed in reactor. This implies the possible mechanisms by which radiation assists the shadow corrosion process; (1) by increasing the electrical and ionic conductivity of the oxide on a Zr alloy, (2) by increasing the oxidizing species at the metal/oxide interface through creating radiolysis products. This project aimed to use the existing spring-loaded wire design shown in Fig. 1 to assess the durability and effectiveness of the newly developed shadow corrosion mitigation coatings on Inconel 718.

In this study, we have demonstrated that spring-loaded Inconel 718 produced a shadow more distinguishable than with previous designs. The shadow region can be clearly identified on the oxide thickness profile. The contact region resulted in a large increase of corrosion rate, with an enhancement of 30-70% compared to the baseline values observed on a reference sample. Various coatings materials applied to the Inconel 718 spring has been tested and their effectiveness on shadow corrosion mitigation has been evaluated.

This research was supported by the AREVA Germany, Contract No.GF01/1016033557.

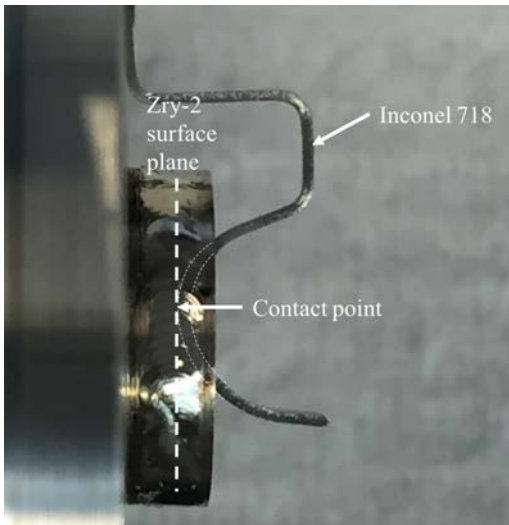


Figure 1. Side view of the new sample design with Spring-loaded Inconel 718 in contact with the Zry-2 sample

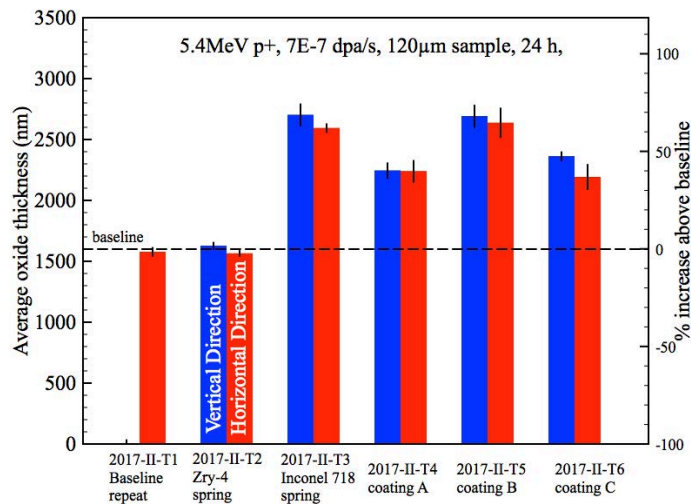


Figure 2. Oxide thickness comparison perpendicular to the Inconel spring.

THE INFLUENCE OF ION IRRADIATION ON THE CORROSION KINETICS OF ZIRCONIUM ALLOYS

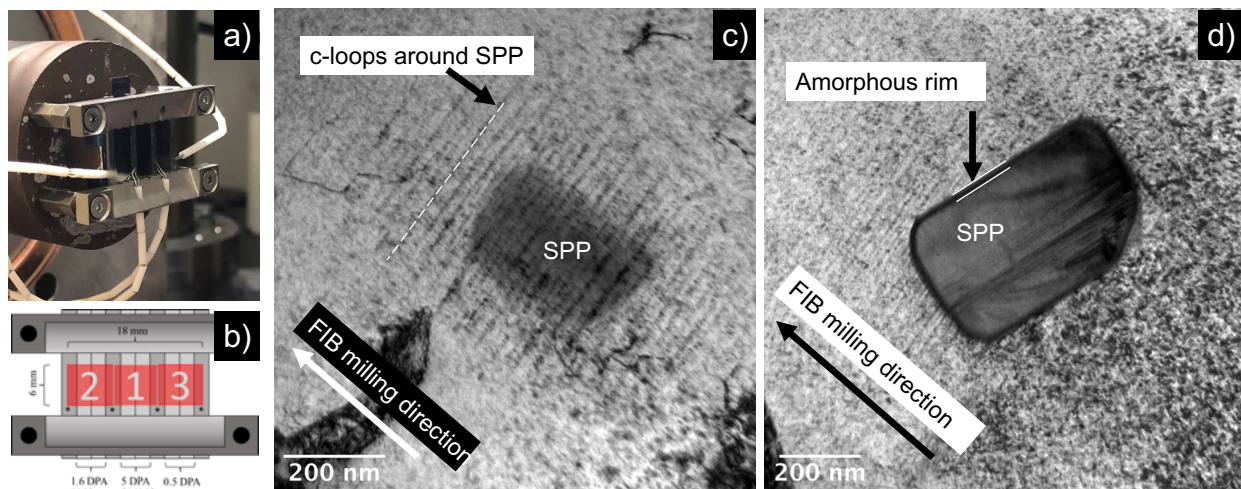
P. Wang¹, G.S. Was¹, B. Kammenzind²

¹Department of Nuclear Engineering and Radiological Sciences, University of Michigan

²Naval Nuclear Laboratory

The mechanistic understanding of zirconium alloy corrosion and hydrogen pickup in out of reactor testing has advanced the state-of-the-art of the field and provided insights in identifying promising alloys for use in reactors under extreme service duty conditions. However, despite similarities between autoclave and in-reactor corrosion that allow the use of unirradiated material information and testing to identify potential alloys for service, processes that occur in the reactor are quantitatively and qualitatively different than those in an autoclave environment. The aim of this project is to combine both ion irradiation (both bulk and in-situ) and advanced characterization techniques to study the effect of irradiation on the corrosion kinetics of zirconium alloys. The research was focused on separate effects testing for the different mechanisms through which irradiation can affect corrosion, namely irradiation induced changes to the base material microstructure and microchemistry, changes to the water chemistry through radiolysis and irradiation effects on the oxide. A set of 2 MeV proton irradiations was carried out on a Zircaloy-4 heat supplied by NNL. Samples with dimension 2×20×1mm were irradiated to a damage level of 0.5, 1.6 and 5 dpa at temperatures ranging from 280-350°C. The irradiation stage is shown in Fig. (a) where 6 samples were separated by 4 dummy bars into 3 groups and each group was irradiated to a different damage level by adjusting the slit positions during the irradiation. The sequence of slit windows is shown in Fig. (b). The post-irradiation microstructure was characterized on FIB liftout samples under TEM, and the observed features were consistent with the neutron irradiated case shown in the literature, e.g. the c-loops around the second phase particles (SPPs) shown in Fig (c), and amorphized rim of the SPPs shown in Fig. (d). A subsequent long-term corrosion exposure will be carried out on these proton-irradiated samples in an autoclave to study the effects of radiation induced microstructure and microchemistry changes on the corrosion behavior of the alloy.

This work was supported by the Naval Nuclear Laboratory.



a) An image of the loaded irradiation stage, b) a schematic of the irradiation sequence and final damage level on each group of samples, c) a SPP with c-loop, and d) a SPP showing amorphized rim.

DOSE RATE EFFECT ON CORROSION OF ZIRCALOY-4 IN PWR PRIMARY WATER USING IN-SITU PROTON IRRADIATION-CORROSION EXPERIMENTS

P. Wang¹, G. S. Was¹, M. Reyes², J. Marian²

¹Department of Nuclear Engineering and Radiological Sciences, University of Michigan

²Department of Mechanical and Aerospace Engineering, University of California Los Angeles

This project aims to understand how irradiation dose rate affects corrosion behavior of zirconium alloy under PWR conditions. In this work, an oxidation kinetics model was developed which accounts for acceleration of oxide layer growth due to irradiation, accompanied by a set of controlled experiments carried out in a corrosion loop coupled to an accelerator beam line for parameterization and validation. Multiple in-situ proton irradiation-corrosion experiments had been conducted to study the effect of damage rate on corrosion rate (as shown in Fig. 1), and the resulting oxide microstructure was also analyzed. The experiments showed an acceleration of corrosion rate of the samples with damage rate, with the growth rate gradually flattening as the damage rate increases. A kinetic model of oxide scale formation and growth in Zircaloy under irradiation that tracks the motion of the oxide/metal interface governed by oxygen diffusion has been developed. The model includes radiation enhanced diffusion (RED) of oxygen in the oxide as the main effect of irradiation and uses the experimental results of oxide layer growth as a function of damage rate to parameterize the RED coefficients as shown in Fig. 2. The scaling of RED coefficient with the irradiation damage rate varies between linear and a square root, depending on whether defect evolution is sink-controlled or recombination-controlled, respectively. The RED manifests itself in two clearly differentiated forms: (i) as a square root dependence of oxygen diffusion coefficient on irradiation damage rate, and (ii) a linear dependence at higher damage rates. A transitional damage rate of 1.1×10^{-6} dpa/s was extracted from our results. We found proton irradiation only affects the pre-transition behavior via this RED coefficient, but not the post-transition regime, and this kinetics model provides a good framework to explain the experimental measurements of oxide growth verses time and growth rate with damage rate.

This research was supported by the Consortium for Advanced Simulation of Light Water Reactors (CASL) under U.S. Department of Energy Contract No. DE-AC05-00OR22725.

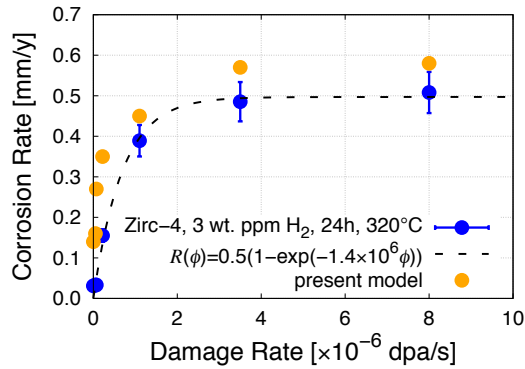


Figure 1. Oxide scale growth rate as a function of damage rate.

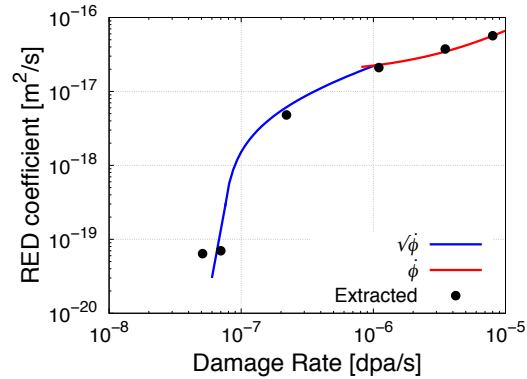


Figure 2. Variation of the radiation enhanced diffusion (RED) with dose rate and fits to two RED models (recombination-controlled regime, $\sqrt{\phi}$, and sink-controlled regime, ϕ).

EFFECTS OF 6 MeV Au ION IRRADIATION ON Cr COATINGS ON ZIRCONIUM ALLOYS

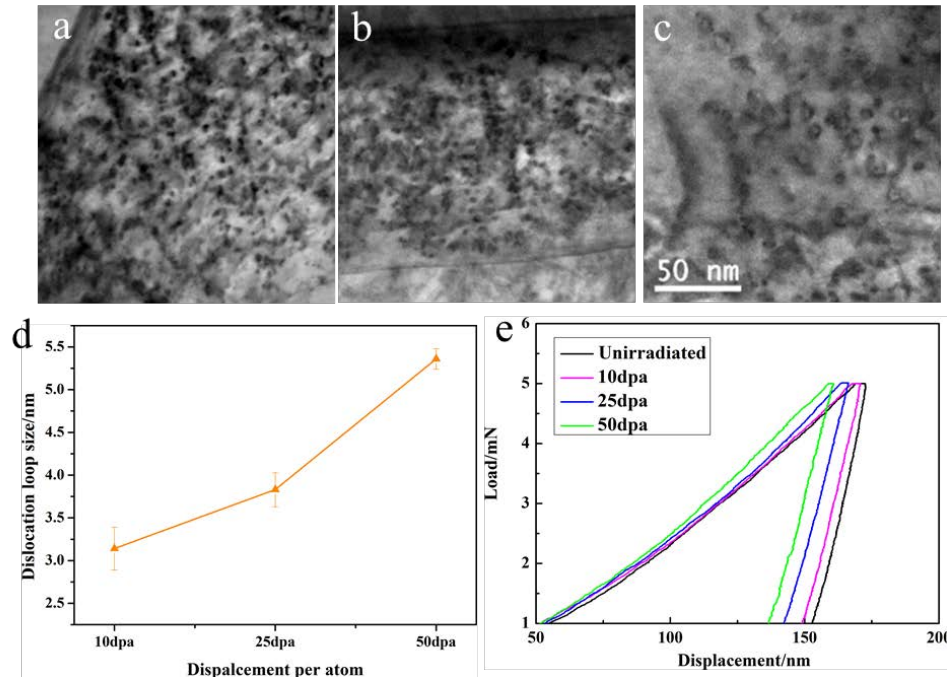
L. Jiang¹, Pengyuan Xiu¹, Chenyang Lu¹, Lumin Wang^{1,2}

¹Department of Nuclear Engineering and Radiological Sciences, University of Michigan.

²Department of Materials Science Engineering, University of Michigan.

In comparison with the conventional nuclear fuel for the light water reactors (LWRs), the Accident Tolerant Fuel (ATF) under development needs to tolerate loss of active cooling in the core for a considerably longer period while maintaining or improving the fuel performance during normal operations. One widely studied ATF concept is to coat the conventional Zr cladding with Cr to improve the corrosion resistance of the cladding at high temperatures.

The goal of this work is to study the behavior of Cr coating on Zr alloys under irradiation. The materials were irradiated at 400 °C with 6 MeV Au ions using Wolverine and Maize accelerators. The regions of around 300 nm depth with a dose 10, 25 and 50 dpa, respectively were chosen for the statistic of loop distribution, in order to avoid the injected interstitial effects. Figures (a-c) below show the BF-STEM images of the irradiated samples. As can be seen, the size of dislocation loops increase with increasing irradiation dose. The quantitative data are shown in figure (d). Results of nanoindentation test prove that irradiation hardening occurs in these coatings, as shown in figure (e). It is worth noting that no voids can be found in all samples.



Microstructure and properties of Cr coatings: (a-c) BF-TEM images of samples irradiated with 10, 25 and 50 dpa respectively (share the same scale bar). (d) Size of dislocation loops versus irradiation dose. (e) Results of nanoindentation test.

PRECIPITATION IN IRRADIATED NI-BASED ALLOYS

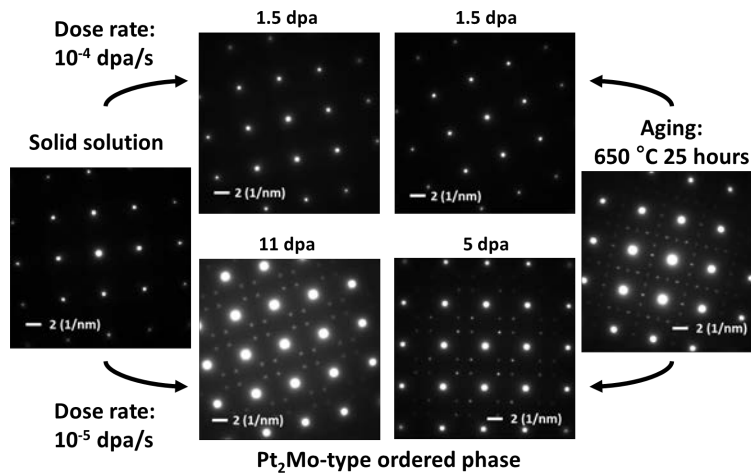
L.-J. Yu, E. Marquis

Department of Materials Science and Engineering, University of Michigan

Ni-based alloys have been used as structural materials for nuclear applications due to their superior high-temperature strength and corrosion resistance. For example, Alloy 625 is already used as control rod components, and Alloy 690 serves as steam generator tubing in light water reactor. However, possible phase transformations in these alloys, including the formation of Pt_2Mo -type ordered phase and the dissolution of strengthening γ'' precipitates can cause degradation of mechanical properties.

Ions and protons have been used as surrogates for neutrons to study the radiation damage in materials. However, the difference in damage rates between these types of irradiation can influence the evolution rate of microstructures or phase stability. To understand the impact of damage rate on microstructural evolution, three commercial Ni-based alloys (Alloys 625, Alloy 625 Plus, and Alloy 690), each with different starting microstructures (solution annealed and aged), were irradiated at 300 °C using 2 MeV proton at the dose rate of 10^{-5} dpa/s, and 5 MeV Ni ion at the dose rate of 10^{-4} dpa/s. The resulting microstructures were characterized using transmission electron microscopy and atom probe tomography. Taking Alloy 625 as an example, the diffraction patterns show that precipitation of a Pt_2Mo -type ordered phase was observed after lower dose rate proton irradiations in both aged and as-quenched samples, while higher dose rate ion irradiations led to complete solid solution regardless of the starting microstructures.

This work is funded by the Department of Energy Nuclear Energy University Program.



[001] zone TEM diffraction patterns of Alloy 625 after various aging and irradiation history.

WAFER-SCALE ION-SLICED LITHIUM NIOBATE THIN FILMS

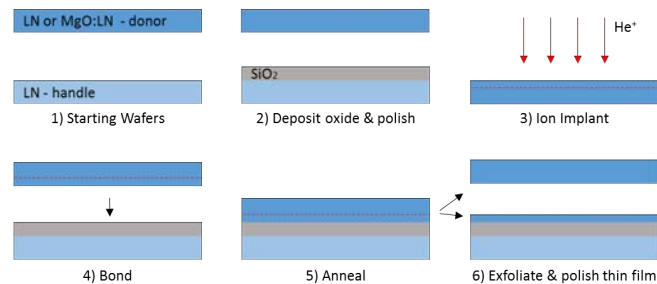
J.T. Nagy, and Ronald M. Reano

Electroscience Laboratory, Department of Electrical and Computer Engineering,
The Ohio State University

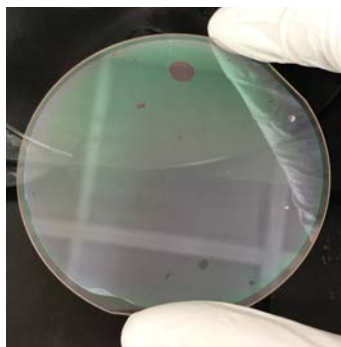
Lithium niobate (LiNbO_3) thin films with sub-micron thickness are useful for on-chip optical devices. These thin films enable waveguides with strong optical confinement, resulting in small and highly efficient devices. The films are ion-sliced from a bulk wafer by implanting with He^+ ions, bonding to a supporting substrate, and a subsequent heat treatment. The ions form a damage layer localized at the implantation depth, which is determined by the ion energy. The heat treatment causes stress at this damage layer and causes a thin film to split off. We have successfully demonstrated ferroelectric domain engineering on these wafers; an important technology in the development of integrated nonlinear optics.

We started with a 3" x 1mm thick 5 mol % magnesium oxide doped lithium niobate wafer which is mounted to a 4" aluminum carrier with colloidal silver paste. The implant dose was $3.5 \times 10^{16} \text{ He}^+/\text{cm}^2$ and the energy was 230 kV. SRIM modeling predicts 230 kV will produce a 820 nm thick LiNbO_3 film. The current density was set to $0.25 \mu\text{A}/\text{cm}^2$ resulting in a total implant time of approximately 6 hours. Thin films were successfully split and the thickness was measured with a Dektak stylus profilometer and found to be near 800nm, in good agreement with simulations. Chemical-mechanical polishing is used to create an optically smooth surface with sub-nm roughness and thin the films to a final thickness of 700 nm.

This material is based upon work supported by the National Science Foundation under Grant No. 1436414



Fabrication process. 3-inch MgO:LN donor wafer and LN substrate (1) are coated with oxide and polished (2). Then the wafers are diced and implanted with He^+ ions at 230 keV (3). The samples are cleaned, bonded (4) and annealed (5). The annealing exfoliates the thin film which is then polished (6).



700 nm thick film bonded to lithium niobate substrate.

MECHANICAL PROPERTY EVOLUTION OF HELIUM IMPLANTED X-750 NICKEL ALLOY USING MICROBENDING TEST

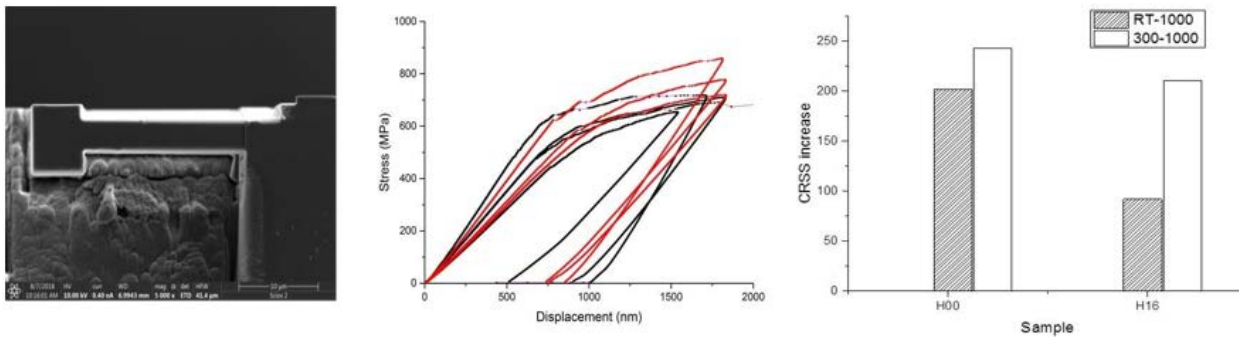
H-H. Jin, I. S. Rye, J.Kwon, G.G.Lee

¹Nuclear Material Research Division, Korea Atomic Energy Research Institute

This work focus on mechanical properties change of X-750 alloys after the helium implantation through micro bending test. The experimental approach in this work is believed to be applied for demonstration of material degradation behavior in irradiated X-750 alloy used for the spacer components. The experimental material in this study is a solution annealed nickel based alloy (Inconel X-750) plate. Some of X-750 alloy were heat treated at 730 °C for 16 hours to emulate one of typical microstructures (the formation of γ') of the annular garter spring spacer component. Helium ions were used in multiple energies ranges, from 1420 keV to 2820 keV, for the development of uniform radiation damage and implanted ion concentration in the ion-implanted samples. It is found that the uniform layer for radiation damage (~ 0.1 dpa) and implantation (~ 1000 appm He) is located in the region ranging from 2 \sim 5 μm in depth.

The average critical resolved shear stress (CRSS) of the micro-cantilever samples before helium implantation was measured to be 300 MPa for as-received X-750 alloy (H00) and, 500 MPa for heat-treated X-750 alloy (H16) respectively. After the multiple energy helium implantation at room temperature, the increase in CRSS value is measured to be approximately 200 MPa for the as-received sample and 100 MPa for the heat-treated X-750 sample respectively. On the other hands, the increase in CRSS value after 300 °C implantation is measured to be approximately 200 MPa for both the samples. The hardening of the heat-treated X-750 alloy after RT implantation is found to be low. The low hardening phenomenon seems to be due to the disordering process of γ' . Further microstructural characterization will be investigated by TEM examination to better understand the effects of irradiation on microstructure and mechanical properties of X-750 alloy.

This work is supported by a National Research Foundation of Korea (NRF) grant funded by the Korea government.



SEM image showing the micro cantilever of helium implanted samples for microbending test (left), Stress - displacement profiles of the as-received (black) and the heat-treated (red) X-750 alloys after helium implantation (center) and the increase in CRSS values estimated from the micro bending test (right).

STUDY OF THE RADIATION INDUCED SEGREGATION EFFECTS IN SILICON CARBIDE

T. Baba¹, H. Zhang¹, X. Wang², I. Szlufarska¹

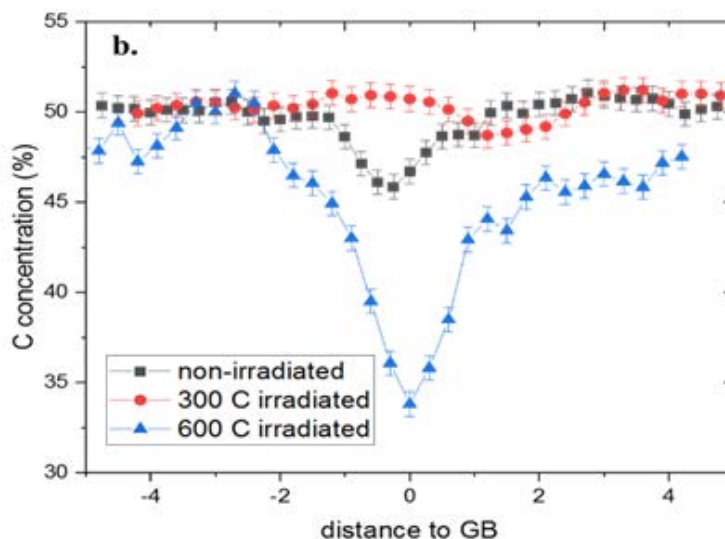
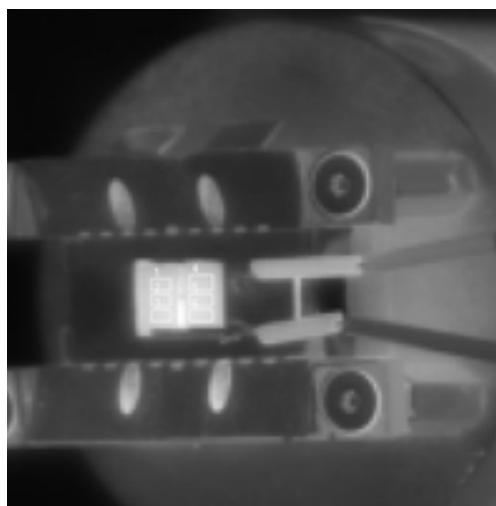
¹Department of Material Science, University of Wisconsin-Madison

²Center for Nanophase Materials Sciences, Oak Ridge National Laboratory

The goal of this study is to examine the radiation effects on the grain boundary of silicon carbide. Radiation-induced segregation (RIS) is one of the most dramatic changes that can take place in the materials under irradiation. The bombardment of high energy particles can generate a large number of point defects, which tend to migrate to defect sinks like grain boundaries (GB). In a multi-component alloy, the preferential diffusion of defects via certain elements can lead to the build-up or depletion of certain elements in the vicinity of defect sinks. RIS can cause substantial changes in structure and chemistry of GBs, and significantly degrade material properties. Systematic studies have been focused on investigating RIS in metallic systems. However, the RIS in ceramics, including SiC, is less understood.

To examine the radiation effects, CVD-SiC samples were irradiated at four different temperatures with 3.15 MeV C-ion at the Michigan Ion Beam Laboratory. Electron energy loss spectroscopy (EELS) spectrum image were collected near GBs and C concentration profiles were obtained. The spectrum was collected using 60 keV Nion UltraSTEM 100 located at the Oak Ridge National Laboratory. The interesting discovery thus far is that the segregation of carbon to the GBs follows a non-monotonic trend with irradiation temperature. This non-monotonic trend of RIS is not observed in metallic alloys. It suggests the RIS theory in metals may not be applicable to covalent systems like SiC, which has more complicated defect kinetics and energy landscape. The further study is in progress with SiC-bicrystal, which resolves some of the experimental difficulties associated with the CVD-SiC samples.

We gratefully acknowledge financial support from Department of Energy - Basic Energy Science Program.



FLIR thermal image of irradiation stage b. carbon concentration profile measured near GB in non-irradiated SiC samples and samples irradiated at 300 °C and 600 °C.

PROTON-IRRADIATED STEEL SPECIMENS FOR CALIBRATION OF A CRYSTAL PLASTICITY MODEL

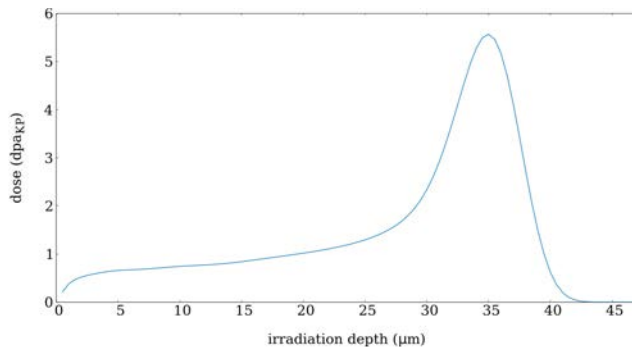
J.-M. Scherer, J. Hure, B. Tanguy
DEN-Service d'Etudes des Matériaux Irradiés, CEA, Université Paris-Saclay,
F-91191, Gif-sur-Yvette, France

In the context of ductile rupture of irradiated face-centered cubic (FCC) materials, the goal of this study is to calibrate a crystal plasticity model through tensile testing of non-irradiated and proton-irradiated AISI 316L single crystal specimens. Pre- and post-irradiation Transmission Electron Microscopy (TEM) observations of the specimens will provide dislocation and Frank dislocation loop densities which are input data of the model. The crystal plasticity model will be calibrated through comparison of the numerical predictions to the experiments.

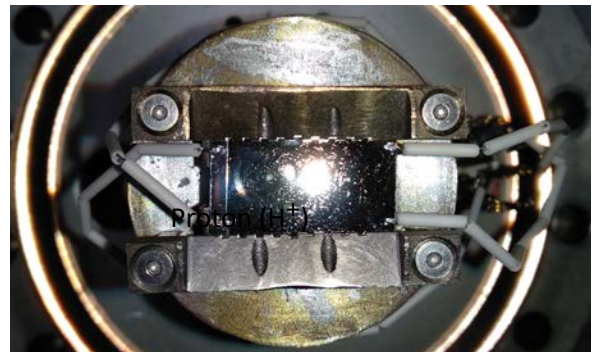
To perform tensile tests on proton-irradiated AISI 316L single crystal specimens, a 0.9 mm thick single crystal plate of area 18mm x 20mm was irradiated over a 10mm x 18mm area. A single irradiation experiment was conducted using Wolverine beamline #2 with a 3 MeV H^+ beam. The figure (a) below shows the damage profile, in which a total dose of 1 displacement per atom (dpa) at 15 nm depth was collected with a total fluence of 3.4×10^{19} ions/cm². Specimen temperature was monitored to 350°C which is the temperature for which the defect microstructure is comparable to a neutron irradiation at 300°C typical of Pressurized Water Reactors (PWR). Temperature control was made with thermal imaging calibrated before irradiation with thermocouples spot-welded outside the irradiation area (see figure (b)). Pressure, temperature and beam currents were recorded during the irradiation experiments.

Tensile specimens will be cut in this plate using a wirecut electric discharge machine. In order to perform the tensile tests on an almost homogeneously irradiated layer only (~30 μm thick, see figure (a)), the non-irradiated layer will be removed by mechanical polishing.

We would like to thank Ovidiu Toader for his valuable help to conduct the irradiation experiments at MIBL. Support of CEA program RMATE is also acknowledged.



a)



b)

Displacements per atom with respect to distance to specimen surface for 3 MeV H^+ in AISI 316L steel calculated by SRIM (a), and irradiation stage with AISI 316L single crystal plate and welded thermocouples (b).

PROTON-IRRADIATION OF TYPE 316L AUSTENITIC STAINLESS STEELS FOR IASCC STUDIES: EVOLUTION OF IRRADIATION-INDUCED SEGREGATION USING ADVANCED ANALYTICAL ELECTRON MICROSCOPY

M.G. Burke, F. Scenini, J.Duff, K. Mukahawi
Materials Performance Centre, University of Manchester, Manchester, United Kingdom

Irradiation-Assisted Stress Corrosion Cracking (IASCC) is a known failure phenomenon for reactor internal components irradiated to high neutron doses in Light Water Reactor (LWR) plants. In particular, austenitic stainless steels grades 304L and 316L are susceptible to IASCC as a result of the interaction between neutron radiation-induced microstructural damage, including nanoscale solute segregation to irradiation-induced defects and grain boundaries, and radiolysis of the reactor coolant.

As part of the EU Horizon 2020 SOTERIA program, three miniature four-point bend specimens manufactured from stainless steel grade 316L were proton-irradiated to 5 dpa at 350°C. Mechanical loading of the samples to constant loads just above the yield stress were performed in a recirculating autoclave at 340°C in deoxygenated water with 2 ppm lithium and 25 cc/kg of dissolved hydrogen. The irradiation-induced microstructural changes have been characterized using advanced analytical electron microscopy at the University of Manchester. Using the FEI Talos F200 S/TEM equipped with Super X (4 Silicon Drift Detectors (SDDs)) for high sensitivity STEM-EDX spectrum imaging analyses, direct evidence of nanoscale segregation of Ni and Si to the irradiation-induced Frank loops, dislocations and nanoscale cavities has been obtained from specially prepared electropolished thin-foil specimens extracted from within the proton-irradiated zone. Further characterization of grain boundary segregation is currently in progress. In addition, the SCC specimens will be characterized in detail to assess the extent of intergranular crack and explore the microstructure ahead of the crack tips via the preparation of site-specific TEM specimens using the FIB.

Acknowledgement: This work has received funding from the Horizon 2020 Euratom research and training programme 2014-2018 under Grant Agreement No. 661913.

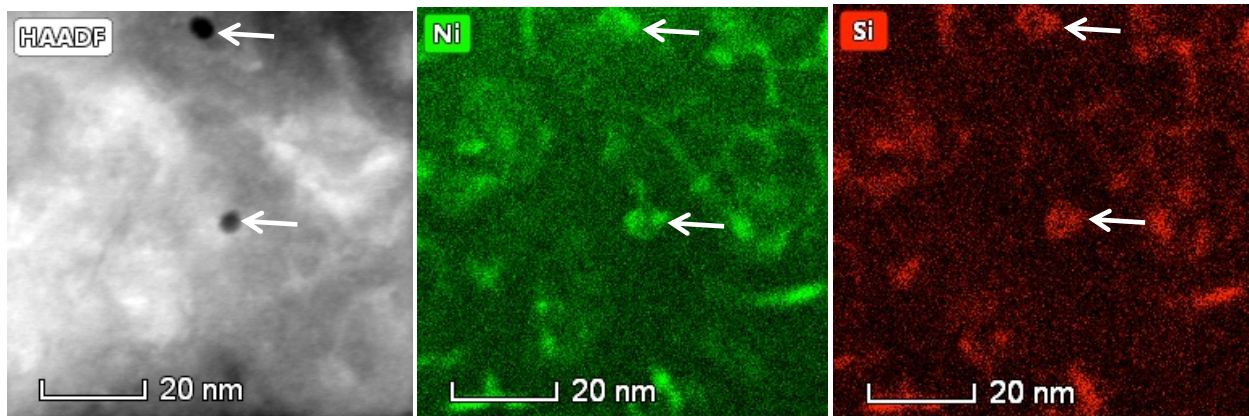


Figure 1. High angle annular dark-field (HAADF) STEM image and corresponding STEM-EDX elemental maps for Ni and Si obtained from the Type 316L specimen proton-irradiated to 5 dpa at 350°C. Note the segregation of Ni and Si to nanoscale cavities (arrowed) and dislocations (out-of-contrast in HAADF image).

TERA-HERTZ SIGNAL GENERATION BY IMPLEMENTING LATERAL PHOTO-DEMBER EFFECT AT GRAPHENE-METAL INTERFACE

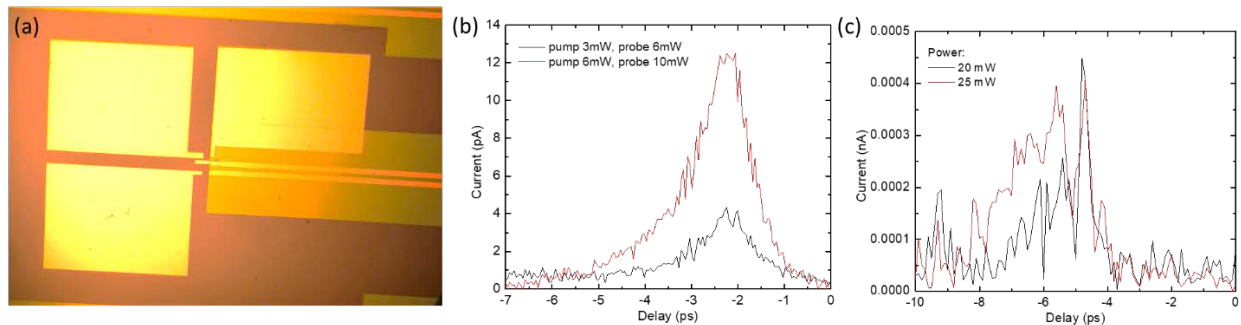
D. Zhang, Z. Xu, T.B. Norris, Z. Zhong

Department of Electrical Engineering and Computer Science, University of Michigan

Tera-Hertz imaging and spectroscopy are promising candidates for chemical detection in health and security applications. However, existing THz sources are limited in energy efficiency and frequency range. The goal of this work is to utilize the lateral photo-Dember process in graphene and make it into a novel THz emitter. The lateral photo-Dember effect is a process of THz emission in materials when a femtosecond laser pulse illuminates the device. Figure (a) shows the device structure. Our device is a graphene transistor with a channel length of $20\ \mu\text{m}$. Two gold contacts with a thickness of $300\ \text{nm}$ were fabricated as the contact. When the pulse hit our device, hot carriers are generated in graphene and create a pico-second scale instantaneous current across the metal-graphene interface. The current leads to emission of THz signal, which is comparable to commercial photoconductive switches based on simulation, which makes it a good candidate as a powerful THz source.

To perform a time-resolved measurement of the THz signal generated from our device, we designed an on-chip pump-probe setup. In the setup the THz emitter is tied to a metal transmission line, Fig (a). The THz signal propagates along the transmission line and gets collected by an Auston switch. The Auston switch has a sub-picosecond response time and provides a good temporal resolution over the THz signal generated. To fabricate the Auston switch, O^+ ions were implanted to a 300-nm -thick layer of undoped silicon on a silicon-on-sapphire (SOS) substrate. The O^+ ions were injected at $100\ \text{keV}$ with a dose of $10^{15}\ \text{cm}^{-2}$. The speed of the switch was tested in a pump-probe setup, where one switch was biased at 10V and illuminated at $3\text{mW}/6\text{mW}$ to produce the THz signal, while the other switch was used to collect the signal. It was verified that it operates at a picosecond speed, Fig. (b). Some preliminary tests over the THz generating device were also performed, showing THz signal generated from the graphene-metal interface. More work is to be performed to increase the SNR in the data collected and to further explore the mechanism of such THz generation process in two dimensional materials.

This work is supported by National Science Foundation (NSF), 1509354.



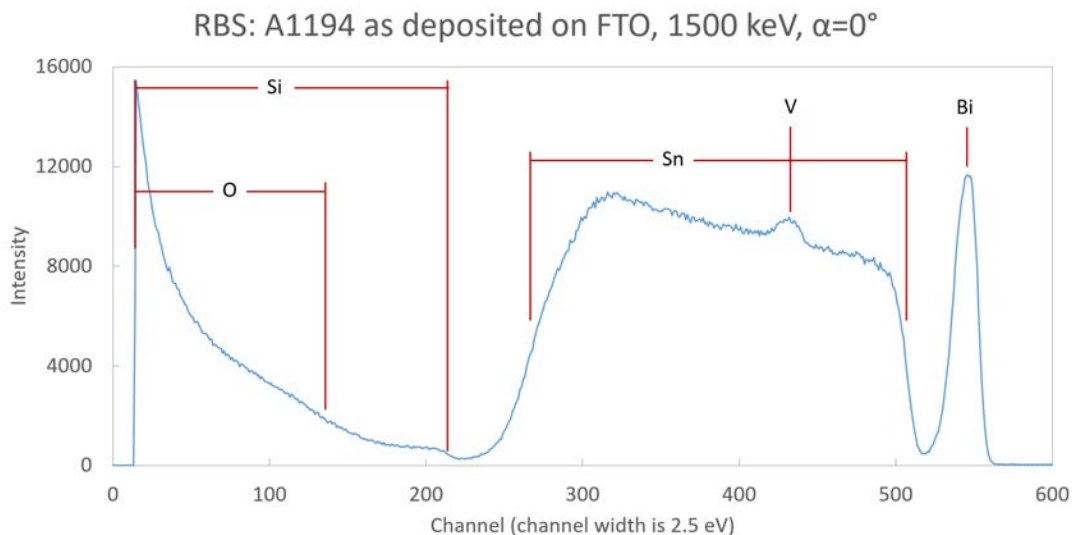
(a) Device structure under optical microscope. (b) Pump-probe measurement over two Auston switches, indicating a pico-second operation speed. (c) THz signal generated in the graphene devices and collected by the Auston switch.

RUTHERFORD BACKSCATTERING SPECTROMETRY OF NANOLAMINATE AND TERNARY OXIDE THIN FILMS

A.R. Bielinski

Bismuth vanadate (BVO) is a mid-bandgap semiconductor of interest to the photoelectrochemistry research community as a photoanode material for solar water oxidation. We developed a process to deposit thin films of BVO using atomic layer deposition (ALD). This is of interest because ALD enables conformal deposition of 3D nanostructures with precise control of thickness and composition. The ALD process for BVO consists of first depositing a nano-laminate of Bi and V oxides and then post annealing to achieve the ternary monoclinic BVO phase. Rutherford backscattering spectrometry (RBS) was explored as a method to probe variations in film composition through the thickness of the film both before and after annealing. Initial studies using x-ray photoelectron spectroscopy (XPS) showed that there might be a Bi-rich surface layer after annealing, but using ion sputtering to depth profile through the film thickness was not possible due to drastically different sputter rates for Bi and V. RBS was of interest as a non-destructive method to understand compositional variations through the film thickness. RBS measurements were performed on BVO films deposited on fluorine doped tin oxide (FTO) glass substrates for samples both as deposited and annealed. The elements of interest: Bi, V, O, Sn, and Si, were detected in the measurement results. However, due to substrate and interfacial roughness, it proved difficult to sufficiently model the full multilayered structure with the precision necessary to extract small differences in composition. The morphology of the annealed film is substrate dependent and FTO, a transparent conductor, is an essential part of the photoanode structure. Attempts to anneal the film on a low roughness substrate, Si, yielded film morphologies that were not representative of the films in the full device. At the time it was deemed more time and cost effective to study the films using transmission electron microscopy (TEM) and energy dispersive x-ray spectroscopy (EDX) rather than developing more extensive modeling efforts to extract the needed information from the RBS spectra. As a result of these experiments, a method to control the film morphology on different substrates has been developed so RBS could conceivably be tried again in the future, if needed.

This work was supported by the National Science Foundation Graduate Research Fellowship Program under Grant No. (DGE 1256260).



Example RBS spectra of the nanolaminate structure of Bi and V oxides. Si and Sn are also present from the substrate.

ION IRRADIATION INDUCED ALPHA PRIME PRECIPITATE FORMATION IN HIGH PURITY Fe-Cr ALLOYS

Y. Zhao¹, A. Bhattacharya², S.J. Zinkle^{1,2,3}

¹Material Science and Engineering Department, University of Tennessee, Knoxville

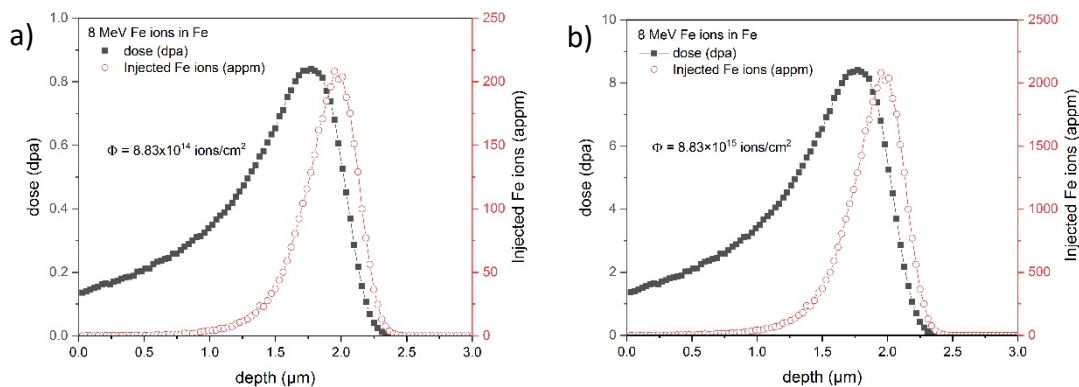
²Materials Science and Technology Division, Oak Ridge National Laboratory, Oak Ridge, TN

³Nuclear Engineering Department, University of Tennessee, Knoxville

Binary Fe-Cr alloys are simple representatives of ferritic-martensitic steels which are structural material candidates for Gen. IV fission and fusion reactors. For Cr levels >8-9% and irradiation temperatures below ~480°C, these alloys suffer from neutron irradiation-induced/enhanced embrittling Cr-rich α' precipitation. However, α' formation in FeCr alloys is rarely reported after high dose rate ion irradiations. The responsible mechanism is uncertain but may involve ballistic dissolution of precipitate nuclei. The goal of this study is to examine the combined effects of dose rate and temperature on the microstructure evolution in these high purity binary alloys with Cr concentration ranging from 0 to 18%. Transmission electron microscope (TEM) and high count rate energy dispersive X-ray spectroscopy (EDX) in scanning TEM mode, will be used to study the formation of α' phase and associated dislocation loop microstructure evolution.

To examine the effects of dose rate and temperature on the microstructural evolution of Fe-Cr alloys, five irradiation conditions are selected at temperatures of 350 - 450°C up to mid-range doses of 0.35 - 3.5 dpa, with dose rates 10^{-4} - 10^{-5} dpa/s, and all of the experiments have been completed. Thin (300-400 μm) disks of 3 mm diameter were prepared. All of the experiments were performed using 8 MeV Fe^{+++} ions. The figure (a) and (b) below show the damage profile, in which total doses of 0.35 or 3.5 displacements per atom (dpa) at 1 μm depth was collected. Temperature control was made with thermocouples, spot-welded on to the Fe-14Cr disks. Pressure, temperature and beam currents were recorded during the irradiation experiments.

This work was supported by the Office of Fusion Energy Sciences, U.S. Department of Energy (grant # DE-SC0006661 with the University of Tennessee and contract DE-AC05-00OR22725 with UT-Battelle, LLC).



SRIM based estimates of depth profile of displacement damage in dpa and implanted Fe ions concentration in pure Fe. (a) 0.35 dpa at mid-range, (b) 3.5 dpa at mid-range.

MICROSTRUCTURAL RESISTANCE OF STRUCTURAL ALLOYS SUBJECTED TO HIGH DOSE, DUAL ION IRRADIATION

C. Lear, M. Wang, M. Song, G.S. Was

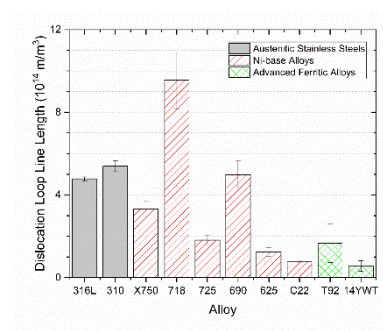
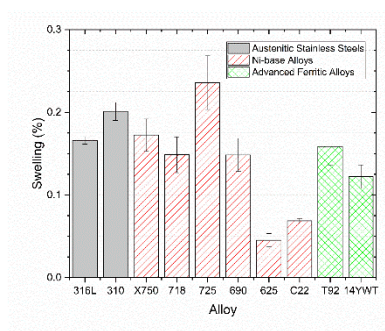
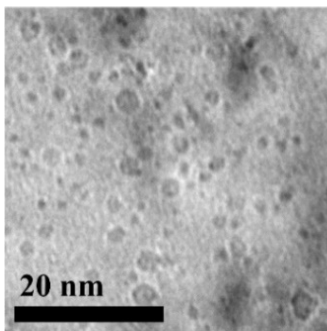
Department of Nuclear Engineering and Radiological Sciences, University of Michigan

The Advanced Radiation Resistant Materials (ARRM) program is tasked with identifying commercial and advanced alloys with superior resistance to radiation induced damage, including changes in microstructure, corrosion, and mechanical properties with irradiation. Helium generation from irradiation-induced transmutation reactions becomes especially important to microstructural evolution at high dose, as vacancy trapping by interstitial He enhances cavity formation and alters the development of dislocations and secondary phases. This year candidate stainless steels (316L and 310), Ni-base alloy (690, 625, C22, X750, 718A, and 725), and advanced ferritic alloys (T92 and 14YWT) were characterized for cavity swelling and dislocation line length (m/m^3) following high dose, dual ion irradiation.

Samples were simultaneously irradiated with 5 MeV self-ions (Fe^{++} or Ni^{++}) and degraded 2 MeV He^{++} ions at the Michigan Ion Beam Laboratory (MIBL), for a dose of 150 dpa and a He content of 10-20 appm He/dpa at 400 °C. Degradation of the He^{++} beam lead to variable implantation depth into the samples, with the final He content varying by $\leq 35\%$ throughout the characterized depth (600-800 nm). Cross-section sample foils were produced from the irradiated alloys for analysis using scanning/transmission electron microscopy (S/TEM).

While cavities were observed throughout the irradiated alloys, swelling was very modest ($< 0.3\%$). Microstructural evolution was least pronounced in the low-Fe Ni-base alloys and the advanced ferritic steels, with the candidate alloys generally performing comparably or better than the 316L stainless steel or Inconel X750 commonly used in industry. Broad agreement was seen with reports of in-reactor irradiated structural materials, demonstrating the capability to rapidly simulate neutron damaged microstructures using dual ion irradiation.

The ARRM program is supported by the Electric Power Research Institute (contracts 10002164 and 10002154) and the U.S. Department of Energy (contract 4000136101).



(Left) Nanoscale cavities, ~ 2 nm diameter, in ferritic alloy 14YWT. (Middle) Cavity swelling induced in austenitic stainless steels (solid black), Ni-base alloys (striped red), and advanced ferritic alloys (cross-hatched green). (Right) Dislocation loop line length induced in the same.

CALIBRATION OF RADIOCHROMIC FILM FOR USE IN LASER-DRIVEN ION ACCELERATION EXPERIMENTS

P.T. Campbell¹, L. Willingale², K.M. Krushelnick¹

¹Department of Nuclear Engineering and Radiological Sciences, University of Michigan

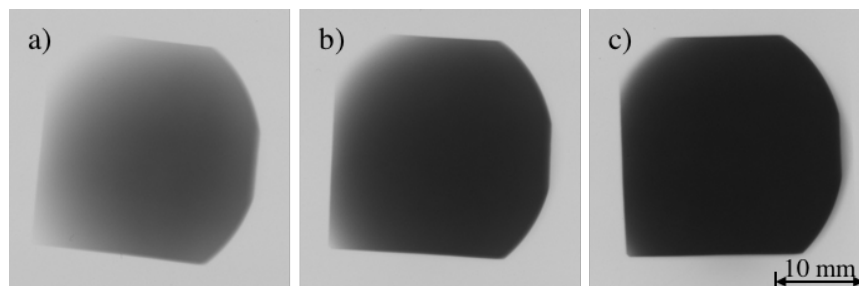
²Department of Electrical Engineering and Computer Science, University of Michigan

The interaction of a high intensity laser pulse with solid foil targets can produce a burst of high energy ions accelerated via the target normal sheath acceleration (TNSA) mechanism [1, 2, 3, 4]. First, the laser pulse excites a population of relativistic electrons which stream through the thin target and establish a strong, electrostatic sheath field on the rear surface. The sheath field can ionize the hydrocarbon contaminant layer on the target's rear surface and accelerate protons and other ions energies of many 10s of MeV. These laser-produced ion beams have a number of unique qualities that make them a particularly attractive source for charged particle radiography [5, 6]. The acceleration occurs over time-scales comparable to the laser pulse duration (typically ranging from 0.1 to 10s of ps). The beam propagation is nearly laminar [7, 8], emanating from the rear of the target as if from a small, virtual source [5]. This quick burst of ions has a quasi-Maxwellian energy spectrum, which can be leveraged to achieve temporal resolution by allowing for time-of-flight dispersion between the source and the radiography subject. All of these features combine to make laser-generated ion beams well suited to diagnose dynamic electric and magnetic fields often present in high energy density (HED) experiments.

Radiochromic film (RCF) is often used for dosimetry of ionizing radiation (such as electrons, photons or protons) in medical, industrial or scientific applications [9]. The film is typically composed of a transparent substrate which is coated with a thin layer of initially transparent dye. Upon irradiation, the dye changes to a bluish color. The optical density, or darkness, of the film after irradiation can be correlated to the dose. To accurately quantify the relative number of ions across the beam profile, the RCF radiation response must be calibrated with a well characterized source.

We proposed an experiment using Wolverine 3MV Pelletron ion accelerator the Michigan Ion Beam Laboratory (MIBL) to irradiate pieces of RCF with known doses of protons. We first attempted to validate the design and calculations with a few test irradiations. The accelerator produced a beam of 5.4 +/- 0.02 MeV protons with a 3 +/- 0.02 nA current. The beam has a FWHM diameter of 2 mm and was raster-scanned over a 20 mm by 20 mm area. Pieces of RCF were cut into 5 cm by 5 cm squares and wrapped in 13 μ m thick aluminum foil to prevent light exposure. The figure shows the results from three test irradiations in which RCF targets were exposed to 1, 10, and 100 s of proton irradiation. The results shown in the figure demonstrate the diagnostic utility of RCF. Immediately after the irradiation, the RCF provides an image of the proton beam spatial distribution without any further chemical treatment or development.

Support for this work provided by the Department of Energy / NNSA under Award Number DE-NA0003606.



Results from three test irradiations: a) 1 second, b) 10 second, and c) 100 second exposure to 3 nA of 5.4 MeV protons. Darker regions correspond to higher proton dose.

EVALUATION OF THIN PLASTIC SCINTILLATOR RESPONSE TO PROTON IRRADIATION

C. Ferretti¹, D. Levin¹, N. Ristow¹, H. Ochoa¹, P. Friedman²

¹Department of Physics, University of Michigan

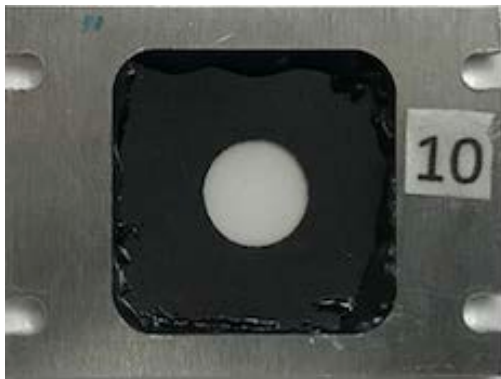
²Integrated Sensors, LLC, Toledo, OH

We have established a program to evaluate the response of thin-plastic scintillating materials to proton radiation. Objectives of the program are threefold: 1) determine light yields for a host of thin plastic scintillating materials (less than 1 mm) during exposure; 2) measurement of the proton beam profiles; 3) measure short-term and long-term radiation damage effects after exposures.

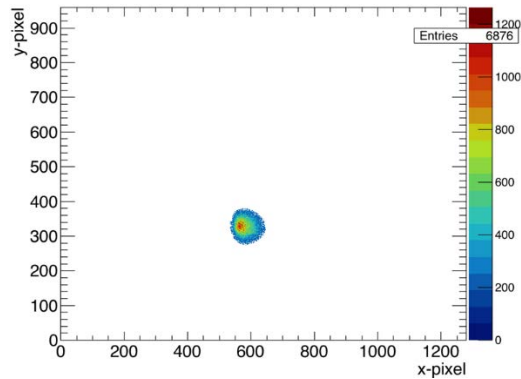
The materials under consideration are samples of aromatic polyesters that exhibit scintillation in the visible spectrum by itself without any additives, and polyvinyltoluenes which use waveshifting fluors. Specimens are held in 2.6 x 3.5 cm square aluminum frames which are mounted on a stage located in the proton beam pipe and centered on the beam axis. An example is shown in figure (a). Light yields and imaging was done using a variety of commercially available photosensors and lensing systems. A beam image is shown in figure (b). Each specimen's scintillation yield was measured before and after proton irradiation, using a photomultiplier tube and UV excitation system configured in a dark box.

This program is ongoing and data are being collected and analyzed. Additional details of the apparatus are currently proprietary and patent pending.

This work was supported by the U.S. National Institutes of Health, National Cancer Institute under Grant No. 5R44CA183437-04, and the Department of Energy, Office of Nuclear Physics under Award No. DE-SC0013292.



(a)



(b)

Scintillator sample (a), and beam spot (b) for 1 ms exposure.

IDENTIFYING DEFECTS AND THEIR ELECTRONIC SIGNATURES IN REGROWN GaN HETEROSTRUCTURES

J. He¹, G. Cheng¹, D. DelGaudio¹, J. Occena¹, F. Naab², R.S. Goldman¹, M. Nami³, B. Li³, J. Han³

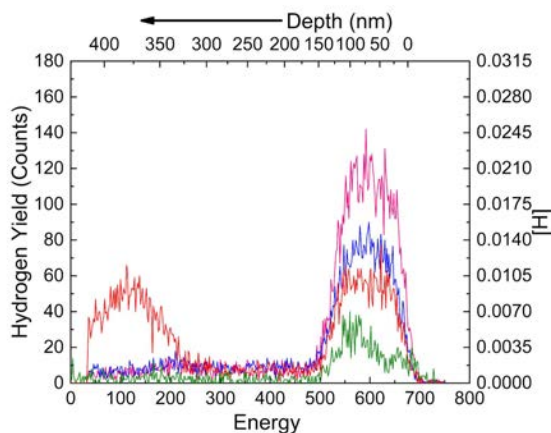
¹Department of Materials Science & Engineering, University of Michigan

²Department of Nuclear Engineering and Radiological Sciences, University of Michigan

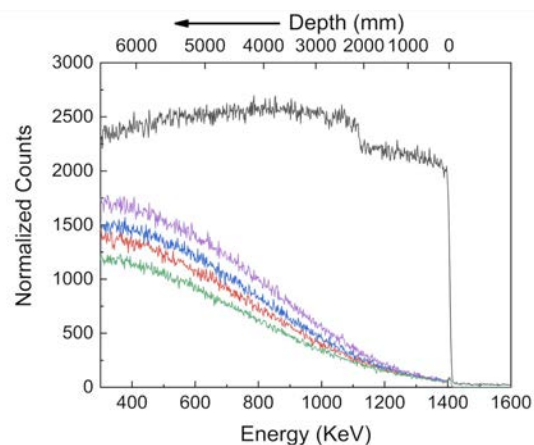
³Department of Electrical Engineering, Yale University

Although silicon-based electronics are used to power light-emitting diodes and electric vehicles, their utility in high power applications is limited by a low breakdown voltage. The most promising alternative power devices consist of vertical GaN devices, which often require regrown active regions. Thus, advances in high power device performance require a detailed understanding of the influence of regrowth processing steps on interfacial defects and their electronic signatures. In this work, we examine a series of GaN p-i-n structures prepared with and without ex-situ ambient exposure and/or chemical etching. To quantify the concentration of various native and extrinsic point defects, we utilize a combination of ion beam analyses in conjunction with x-ray diffraction. For all samples, channeling Rutherford backscattering spectroscopy data reveals minimum yield values < 2%, with displaced atom densities ranging from 0.1 to 4 x 10²⁰/cm³. Elastic Recoil Detection Analysis (ERDA) data reveals enhanced [H] near the surfaces of all samples, along with enhanced [H] at the etched/regrown interface. For all samples, cathodoluminescence spectroscopy reveals the GaN near-bandedge and donor-acceptor pair luminescence. For all samples, GaN near-band-edge emission at 3.35 eV and donor-acceptor pair (DAP) emission at 2.85 eV are apparent. Among all samples, "in-situ" exhibits the most intense DAP emission, which indicates the highest amount of Mg in the sample. Meanwhile, the yellow luminescence (YL) at 2.19 eV is only observed in "ex-situ" and "etched/regrowth", while the infrared luminescence (IRL) at 1.47eV is only observed in "in-situ".

This work is supported by ARPA-E AED0000191 and the Michigan Ion Beam Laboratory.



Channeling RBS data: normalized counts vs. Energy and depth (top x-axis), for "in-situ" (pink), "ex-situ" (blue), "etched" (red), in comparison to the random (black) and channeling (green) data for the GaN substrate (green). The RBS data suggests that "etched" has the highest crystalline quality.



ERDA data, consisting of hydrogen counts vs. Energy and depth (top x-axis), for "in-situ" (pink), "ex-situ" (blue), "etched" (red), and the GaN substrate (green). The ERDA data suggests that "in-situ" has the highest [H].

DESIGN OF HIGH ENTROPY ALLOYS (HEAs) FOR NEXT GENERATION NUCLEAR REACTORS

S. Williams, J. Reeder, S. Sheikh

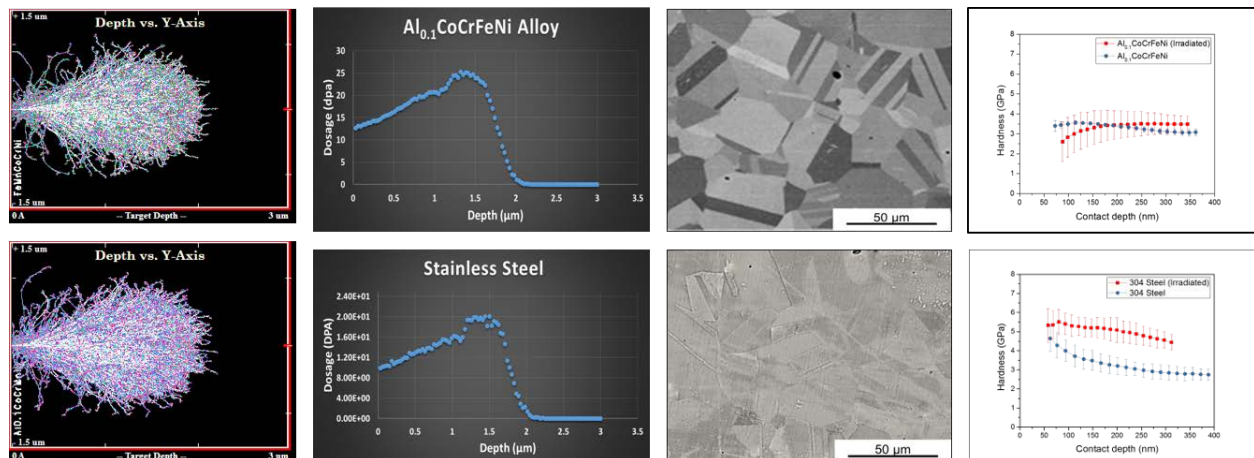
Faculty Advisor: Dr. Sundeep Mukherjee

Dept of Materials Science and Engineering, University of North Texas

Due to the degradation of materials exposed to radiation, parts within a nuclear reactor need to be repaired frequently, which is expensive, unsafe, and leads to downtime. Therefore, there is a growing demand for irradiation resistant alloys for next generation nuclear reactors. High entropy alloys (HEAs) represent a new alloy design strategy that are being considered due to their exceptional mechanical properties and oxidation/corrosion resistance. For this work, two different HEAs were considered namely, CoCrFeMnNi and Al_{0.1}CoCrFeNi. Their irradiation response was compared with stainless steel. Characterization techniques used included scanning electron microscopy (SEM), X-ray diffraction (XRD) and nano-indentation hardness test before and after irradiation as well as SRIM simulation. The results showed that the HEAs were more irradiation resistant than the stainless steel.

Results for the Monte Carlo simulation called Stopping Range of Ions in Matter (SRIM) are shown in Figure 1 for the Al_{0.1}CoCrFeNi HEA compared to stainless steel. The HEA shows lesser damage level and lower DPA compared to the steel. The two HEAs were arc melted and cast in copper mold. They were heat treated at 900 degrees Celsius for 24 hours to obtain equiaxed grains. The Scanning Electron Microscopy (SEM) images for the HEA and steel are also shown in the figure. The HEAs showed lot of annealing twins in the equiaxed microstructure, which is typical for low stacking fault energy materials. There was no change in crystal structure for the HEA, which was single-phase face centered cubic (FCC).

Irradiation experiments were carried out at room temperature using Ni⁺⁺ with an integrated fluence of 1.08 x 10¹⁷ ions/cm². The beam energy was 4.4 MeV at an average sample current of 0.75 μm. All experiments were run without any interruption. Nano-indentation hardness before and after irradiation are shown in the figure below. The Al_{0.1}CoCrFeNi HEA showed negligible change in hardness while stainless steel showed significant irradiation induced hardening. This supported the superior irradiation resistance of the HEA compared to conventional materials.



SRIM results, DPA levels, SEM microstructure, and nano-indentation results for Al_{0.1}CoCrFeNi HEA (top row) compared to stainless steel (bottom row).

EFFECT OF IRRADIATION ON THE STRESS CORROSION CRACKING SUSCEPTIBILITY OF D9

C. R. Lear, G. S. Was

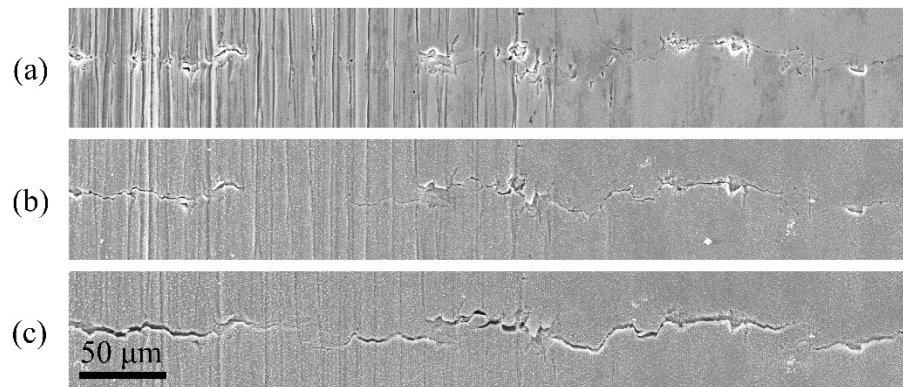
Department of Nuclear Engineering and Radiological Sciences, University of Michigan

The objective of this project was to determine the stress corrosion cracking susceptibility of austenitic stainless steel alloy D9 following ion proton irradiation. As-forged and proton irradiated tensile samples of D9 steel were subjected to microstructural analysis and autoclave straining. Proton irradiation was conducted at 360°C and a damage rate of $\sim 1.6 \times 10^{-5}$ dpa/s to 3 dpa using 2 MeV protons. Slow strain rate testing (SSRT) was performed in a simulated boiling water reactor (BWR) normal water chemistry (NWC) environment. Samples were strained at a rate of $\sim 10^{-7}$ s⁻¹ to 4% plastic strain for all samples and then to 7% for the unirradiated sample.

The stress-strain behavior of the samples revealed possible variations in bulk mechanical properties, verified by microhardness testing, with yield strengths ranging from 633 to 723 MPa. Pre-existing defects appeared to play a significant role in at least one sample, with a marked loss of strength between SSRT experiments. While TiC inclusions fractured at plastic strains as low as 1%, irradiation-assisted stress corrosion cracking (IASCC) was not evident in this D9 steel. Indeed, only two intergranular cracks (~ 5 μ m long) were observed, with these forming in the unirradiated material after 7% plastic strain.

Irradiation-induced microstructural features after a dose of 3 dpa were comparable to previous studies of proton irradiated austenitic steels, including small, relatively dense dislocation loops (12.9 nm diameter, 2.2×10^{22} m⁻³) and an absence of voids. While irradiation induced precipitation of the γ' phase (reported for other proton irradiated austenitic steels) was not observed, irradiation enhanced precipitation of TiC within grains remains inconclusive.

Support provided by Idaho National Laboratory under contract # C0204315.



Evolution of pre-existing defects in sample CN64 (3 dpa proton irradiated) across (a) 0%, (b) 1%, and (c) 4% plastic strain (applied in the vertical direction).

CALIBRATION OF THE DEPOSITION RATE OF A SPUTTER SYSTEM

A. Ansari¹, A. Sarracino¹, B. Torralva², S. Yalisove^{1,3}

¹Department of Applied Physics, University of Michigan

²Department of Climate and Space Sciences, University of Michigan

³Department of Materials Science and Engineering, University of Michigan

When depositing a thin film onto a substrate by sputtering, it is important to know the deposition rate of the system in order to accurately create a film of the desired thickness. To calibrate the deposition rate with an extremely high accuracy, a measuring technique of sufficiently high sensitivity and low error is preferred. Rutherford Backscattering Spectrometry (RBS) was used to measure the thickness of the films, as it is a technique with a low relative uncertainty.

A 2 MeV beam of helium ions was incident on the nickel (Ni) films that were grown. A detector was placed at an angle of 165° relative to the incoming beam, and backscattered ions were collected. After the data was collected for three films that had differing deposition times, SIMNRA was used to model and fit for the thickness of the films. Features from the substrate, borosilicate glass, were observed. A sputtering rate of 0.161 nm/s was calculated.

This work is sponsored by the Air Force Office of Scientific Research Contract Number FA9550-16-1-0312.

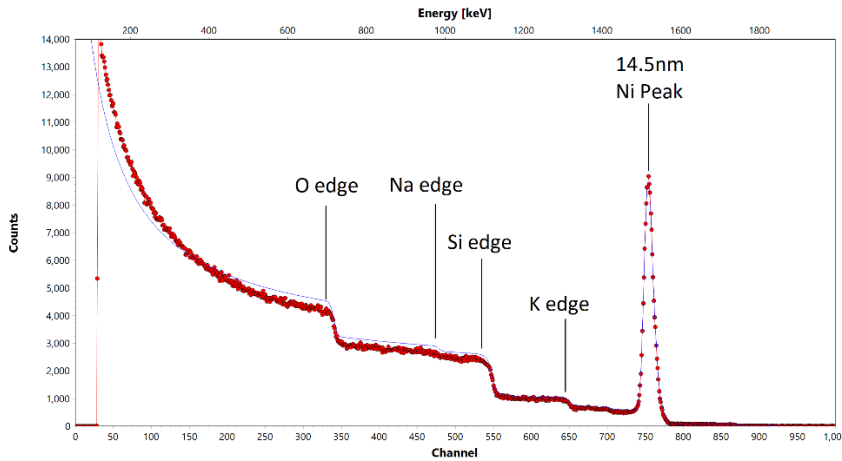


Figure 1. An RBS spectrum with an accompanying fit obtained from SIMNRA. The thickness of the peak as well as the concentrations of other elements were extracted.

Sputter Time (s)	Thickness (nm)
120	14.5
300	42.4
600	91.5

Figure 2. The thickness values extracted from the RBS spectra for three different sputtering growth times.

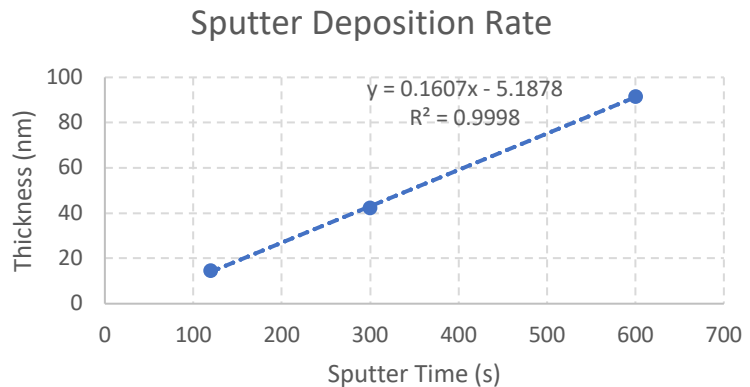


Figure 3. A plot of the thicknesses as a function of sputtering time. A linear fit gives the deposition rate of 0.16 nm/s after a 5s delay.

PROFILING CARBON IN FE-CR ALLOYS USING NUCLEAR REACTION ANALYSIS

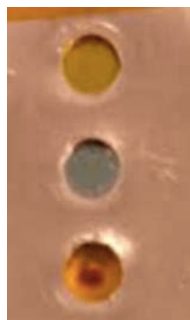
F. Naab, G. S. Was

Department of Nuclear Engineering and Radiological Sciences, University of Michigan

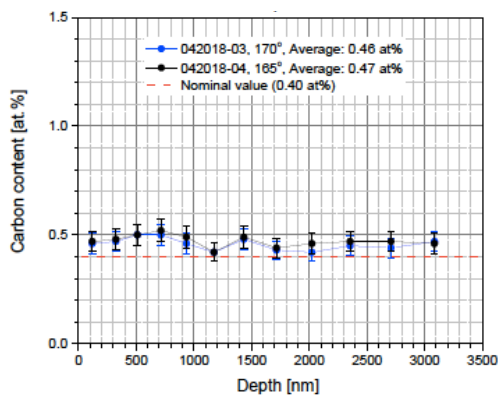
Fe-Cr alloys such as HT9 or T91 are candidates for both fusion and fission systems. In the latter, their application would be in fuel cladding and ducts that will reach damage levels of 200 dpa by end of life. Thus, ion irradiation (self- or heavy-) is typically used as a surrogate for neutron irradiation to gain an understanding of the response of these alloys to high dpa levels. Most all labs have observed the incorporation of carbon in samples irradiated with self ions at high temperature. In fact, this phenomenon has been known for decades, but it becomes a particularly severe problem in self-ion irradiations in which the damage zone is less than 2 μm . While techniques have been developed to mitigate the contamination problem, it is important to have a technique that allows rapid and accurate assessment of the carbon profile through this thickness.

An international round robin is being conducted through the International Atomic Energy Agency (IAEA) to determine 1) the agreement between multiple laboratories on the irradiated microstructure of Fe-9Cr irradiated at 445°C to 35 dpa with 5 MeV Fe^{2+} ions, and 2) to determine whether these irradiations conditions can mimic irradiation in BOR-60 at a temperature of $\sim 400^\circ\text{C}$ and to the same dpa. Nuclear reaction analysis using the $^{12}\text{C}(\text{d,p})^{13}\text{C}$ reaction was used to profile the carbon concentration over the depth of penetration of the self-ion irradiation for each of the participants in the round robin exercise. The figure shows the holder for the Fe-Cr sample (middle position) and two examples of carbon profiles in the sample. The first shows no increase in the carbon level from that in the alloy (0.4 at%), while the second shows a significant increase in the first 2000 nm indicating the incorporation of carbon during the irradiation. Results indicate that mitigation strategies are required to avoid the pickup of carbon during self-ion irradiation.

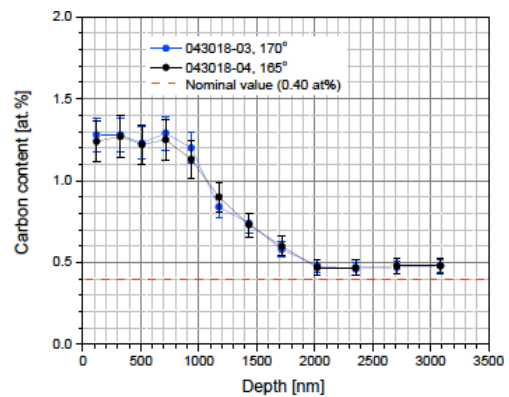
Support provided by the International Atomic Energy Agency.



(a)



(b)



(c)

Sample holder with 3 mm disk sample in the center position (a), and carbon concentration profiles showing no change in carbon following irradiation (b) and significant increase in carbon near the surface of the sample (c).

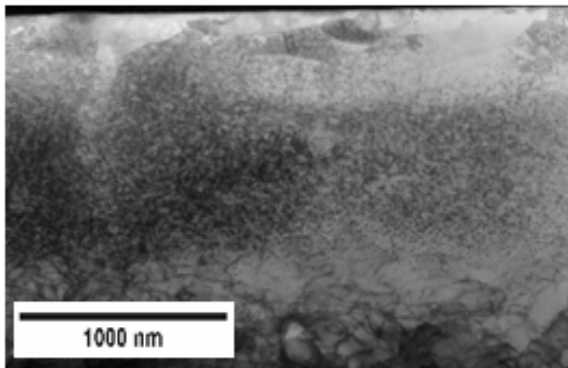
EVOLUTION OF DISLOCATION LOOPS IN RADIATED FeCrAl ALLOYS AT 400°C AS A CANDIDATE CLADDING MATERIAL FOR ATF

P. Xiu¹, L. Jiang¹, C. Lu¹, L. Wang^{1,2}

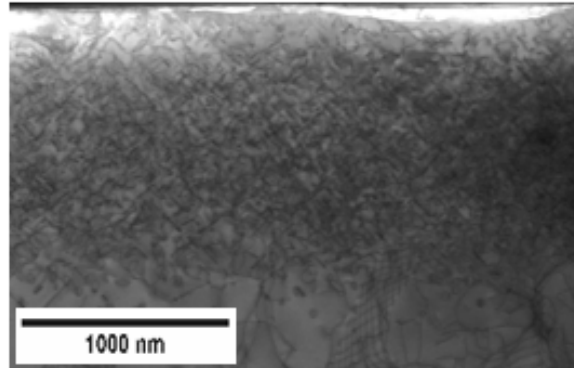
¹Department of Nuclear Engineering and Radiological Sciences, University of Michigan

²Department of Materials Science and Engineering, University of Michigan

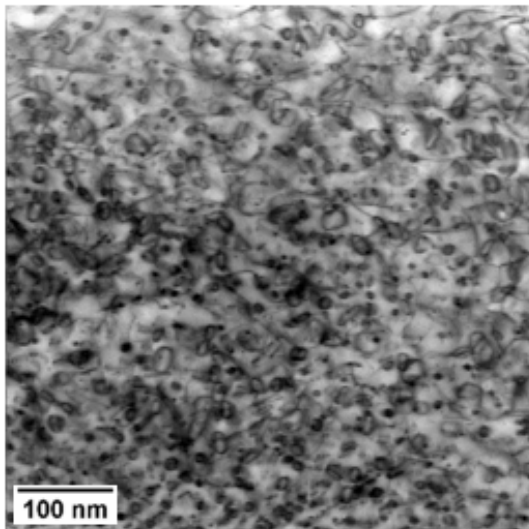
FeCrAl alloys are considered as a candidate accident tolerant fuel (ATF) cladding material for light water reactor (LWR) applications. The addition of Cr and Al gives significantly improved oxidation resistance to the alloys so that the material can survive under extreme environments including high temperature and high irradiation dose. The goal of this work is to examine the dislocation loop evolution with the increase of irradiation dose. 6 MeV gold ions were used to irradiate FeCrAl alloys (nine samples with varying compositions) at 400°C to reach 10 dpa and 25 dpa damage level at 300 nm depth from the surface. Cross-sectional STEM bright-field images below show the irradiation induced damage band in the FeCrAl alloy after 6MeV gold irradiation to 10dpa and 25dpa at 400 °C, respectively. The damage band contains dislocation loops with no voids. The loop size increased significantly with the increasing dose. These alloys will be further irradiated up to 100 dpa with various temperatures for a better understanding of their radiation tolerance.



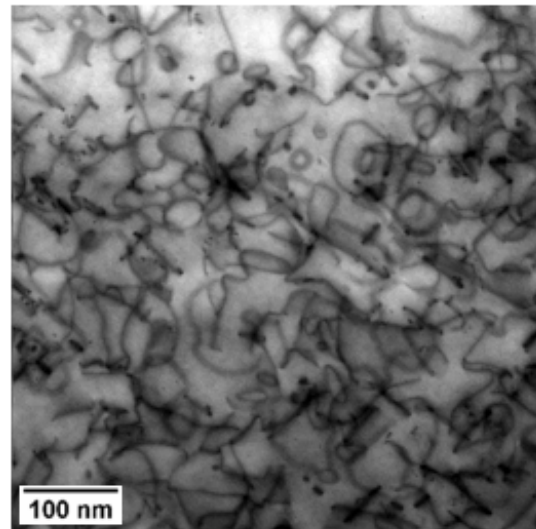
(a)



(b)



(c)



(d)

Cross-sectional STEM bright-field image of FeCrAl after 6MeV gold irradiation to (a) 10dpa (b) 25dpa at 400 °C. Loop images enlarged for (c) 10 dpa and (d) 25 dpa.

EFFECTS OF Au ION IRRADIATION TO MOLYBDENUM ALLOYS AT 400 °C AS A CANDIDATE CLADDING MATERIAL FOR ATF

P. Xiu¹, L. Jiang¹, C. Lu¹, L. Wang^{1,2}

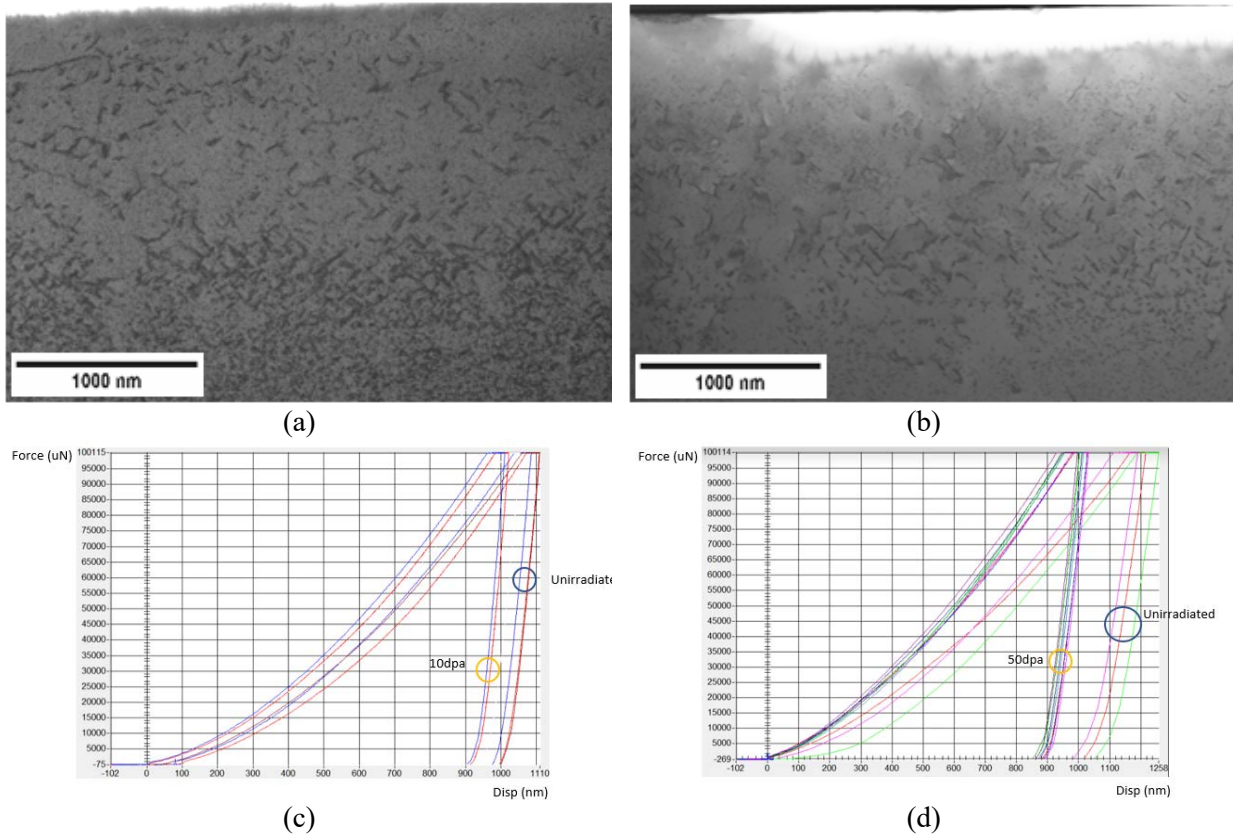
¹Department of Nuclear Engineering and Radiological Sciences, University of Michigan

²Department of Materials Science and Engineering, University of Michigan

Molybdenum alloy (Mo) are considered as a candidate cladding material for the accident tolerant fuel (ATF) of light water reactor (LWR) applications because it is one of the refractory materials that have excellent high temperature oxidization resistance, a highly desired property compared to conventional zirconium alloys. The goal of this work is to examine the irradiation effects of several Mo alloys of various composition with increasing irradiation dose. 6 MeV gold ions were used to irradiate Mo alloys at 400°C to reach 10 dpa, 25 dpa and 50 dpa damage levels at 300 nm depth from the surface.

The cross-sectional STEM bright-field image below shows the irradiation induced damage band in the Mo alloy after 6MeV gold irradiation to 10 dpa and 25 dpa at 400 °C, respectively. Loading-unloading curves from nano-indentation with maximum force of 100mN at 10 dpa and 50 dpa vs un-irradiated region are also shown below to reflect the irradiation hardening effect.

Currently the microstructure of 50dpa are also being analyzed. In the future, Mo alloys will be irradiated at varying temperatures and/or with helium implantation, and the effect of irradiation temperature, dose, and implanted helium will be studied systematically.



Cross-sectional STEM bright-field image of Mo alloy after 6MeV gold irradiation to (a) 10dpa (b) 25dpa at 400 °C; Loading-unloading curve of nano-indentated bulk material at (c) 10dpa and unirradiated area (d) 50 dpa and unirradiated area.

Teaching

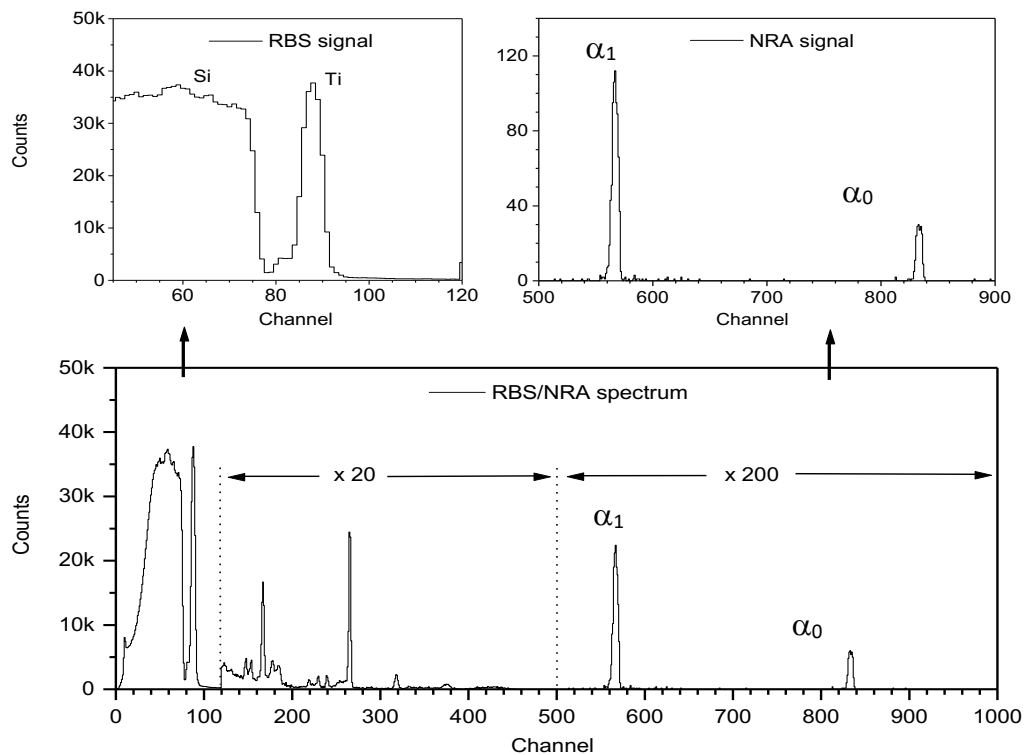
NERS 425 LABORTORY ON NUCLEAR REACTION ANALYSIS

M. Atzmon, F. Naab and O. Toader

Department of Nuclear Engineering and Radiological Sciences, University of Michigan

For one of the modules in the NERS 425 course, students conducted an experiment to determine the stoichiometry of a Ti_xN_y sample using the reaction between a deuterium particle and a nitrogen nucleus: $N^{14}(d,\alpha)C^{12}$. Nuclear reaction analysis (NRA) is a well-established surface analysis technique. In this method, an energetic particle (deuterium – produced by the Tandem accelerator at MIBL) interacts with the nucleus of an N atom in the target to give a reaction product (α particle) that can be measured. The students also use the backscattered yield from an RBS experiment to determine the amount of Ti in the sample by implementing simulation codes like RUMP or SIMNRA with the given experimental spectrum.

In the first meeting, prior to the experiment, a short tutorial was given to the students on the accelerator, electronics, detectors, software, and vacuum components. After that, they worked independently with just the basic support from the MIBL staff (required in the setup of the ion beam and the collection of the spectra). The students decided on a few parameters of the experiment (beam energy, time for spectrum acquisition, etc.), and obtained spectra similar to the ones in the figure.



Typical RBS/NRA spectrum for the TiN film obtained during class.
Conditions: beam energy: 1.4 MeV D^+ , solid angle 5 msr., detector angle 150° .

PUBLICATIONS AND PRESENTATIONS

Publications

1. A. M. Monterrosa, D. Woodley, Z. Jiao, G. S. Was, "The Influence of Carbon on Cavity Evolution in Ion-irradiated Ferritic-martensitic Steels," J. Nucl. Mater. 509 (2018) 722-735.
2. X. Lin, Q. Peng, E-H. Han, W. Ke, C. Sun, Z. Jiao, "Irradiation-induced segregation at phase boundaries in austenitic stainless steel weld metal," Scr. Mater. 140 (2018)11-15.
3. A. M. Monterrosa, Z. Jiao, G. S. Was, "The Influence of Helium on Cavity Evolution in Ion-irradiated T91," J. Nucl. Mater. 509 (2018) 707-721.
4. M. Song, C. R. Lear, C. M. Parish, M. Wang, G. S. Was, "Radiation Tolerance of Commercial and Advanced Alloys for Core Internals: A Comprehensive Microstructural Characterization," J. Nucl. Mater. 510 (2018) 396-413.
5. M. Song, Y. Yang, M. Wang, W. Kuang, C. Lear, G. S. Was, "Probing Long-Range Ordering in Nickel-base Alloys with Proton Irradiation," Acta Mater. 156 (2018) 446-462.
6. Z. Jiao, S. Taller, K. Field, G. Yeli., M. P. Moody, G. S. Was, "Microstructure Evolution of T91 irradiated in the BOR60 Fast Reactor," J. Nucl. Mater. 504 (2018) 122-134.
7. Z. Jiao, J. Michalicka, G.S. Was, "Self-ion Emulation of High Dose Neutron Irradiated Microstructure in Stainless Steel," J. Nucl. Mater. 501 (2018) 312-318.
8. Z. Jiao, J. Hesterberg, G. S. Was, "Effect of Post-Irradiation Annealing on the Irradiated Microstructure of Neutron-Irradiated 304L Stainless Steel," J. Nucl. Mater. 500 (2018) 220-234.

Presentations

1. "Ion Irradiation as a Surrogate for Reactor Irradiation: The Expected and the Surprises – Phenomena that need the help of the modeling community," Multiscale Modeling of Materials (MMM 2018), Osaka, Japan, November 2018.
2. "Insights into the Mechanism of Irradiation Assisted Stress Corrosion Cracking," NuMAT – The Nuclear Materials Conference, Seattle, WA, October 2018.
3. "Ion Irradiation and Fusion Prototypic Neutron Sources," Fusion Prototypic Neutron Source Workshop, U.S. DOE, Gaithersburg, MD, August 2018.
4. "Use of Ion Irradiation to Simulate Radiation Damage from Neutrons," International Nuclear Target Development Conference, Lansing, MI October 2018.
5. "Challenges in Simulating Neutron-induced Radiation Damage using Ion Beams," CIMTEC, Perugia, Italy, June 2018.
6. Contributions of Ion Irradiation to our Understanding of Microstructure Evolution in Reactor," Austenitic Stainless Steels in, Future of Nuclear Materials, Yokosuka, Japan, May 2018.
7. "History of IASCC in the ICG-EAC," International Cooperative Group – Environmental Assisted Corrosion, Knoxville, April 2018.

8. "Evaluation of Microstructure Evolution in Neutron and Ion Irradiated FM Alloys," Microscopy of Irradiation Damage, Oxford, England, March 2018.
9. "Common Mechanism of High Temperature Stress Corrosion Crack Initiation among Austenitic Alloys," Annual TMS Meeting, Phoenix, March 2018.
10. "Comparison of Microstructure Evolution in Neutron and Ion Irradiated FM Alloys," Annual TMS Meeting, Phoenix, March 2018.
11. "Key Factors Driving Crack Initiation in Irradiated Stainless Steel," Keynote talk at Plasticity 2018, Puerto Rico, January 2018.
12. M. Wang, M. Song, G. S. Was, "Stress Corrosion Cracking Behavior of Alloy 718 Subjected to Various Thermal Mechanical Treatments in Primary Water," Proc. 18th International Conference on Environmental Degradation of Materials in Nuclear Power Systems – Water Reactors, The Minerals, Metals & Materials Society, ISBN 978-3-319-67243-4, 2018, 293-305.
13. W. Kuang, M. Song, C. M. Parish, G. S. Was, "Microstructural Study on the Stress Corrosion Cracking of Alloy 690 in Simulated Pressurized Water Reactor Primary Environment," Proc. 18th International Conference on Environmental Degradation of Materials in Nuclear Power Systems – Water Reactors, The Minerals, Metals & Materials Society, ISBN 978-3-319-67243-4, 2018, 535-545.
14. J. Michalicka, Z. Jiao, G. S. Was, "Radiation Induced Precipitates in a Self-Ion Irradiated Cold-Worked 316 Austenitic Stainless Steel Used for PWR Baffle Bolts," Proc. 18th International Conference on Environmental Degradation of Materials in Nuclear Power Systems – Water Reactors, The Minerals, Metals & Materials Society, ISBN 978-3-319-67243-4, 2018, 565-580.
15. P. Wang, G. S. Was, "In-Situ Proton Irradiation-Corrosion Study of ATF Candidate Alloys in Simulated PWR Primary Water," Proc. 18th International Conference on Environmental Degradation of Materials in Nuclear Power Systems – Water Reactors, The Minerals, Metals & Materials Society, ISBN 978-3-319-67243-4, 2018, 245-258.
16. K. K. Mandapaka, G. S. Was, "Corrosion of Multilayer Ceramic-Coated ZIRLO Exposed to High Temperature Water," Proc. 18th International Conference on Environmental Degradation of Materials in Nuclear Power Systems – Water Reactors, The Minerals, Metals & Materials Society, ISBN 978-3-319-67243-4, 2018, 281-292
17. M. Song, M. Wang, G. S. Was, L. Nelson, R. Pathania, "Irradiation Assisted Stress Corrosion Cracking (IASCC) of Nickel-Base Alloys in Light Water Reactor Environments – Part I: Microstructure Characterization," Proc. 18th International Conference on Environmental Degradation of Materials in Nuclear Power Systems – Water Reactors, The Minerals, Metals & Materials Society, ISBN 978-3-319-67243-4, 2018, 949-960.
18. M. Wang, M. Song, G. S. Was, L. Nelson, R. Pathania, "Irradiation Assisted Stress Corrosion Cracking (IASCC) of Nickel-Base Alloys in Light Water Reactor Environments – Part II: Stress Corrosion Cracking," Proc. 18th International Conference on Environmental Degradation of Materials in Nuclear Power Systems – Water Reactors, The Minerals, Metals & Materials Society, ISBN 978-3-319-67243-4, 2018, 961-972.
19. Y. Chen, Y. Dong E. Marquis, Z. Jiao, J. Hesterberg, S. Was, P. Chou, "Solute Clustering in As-irradiated and Post-irradiation and Annealed 304 Stainless Steel," Proc. 18th International Conference

- on Environmental Degradation of Materials in Nuclear Power Systems – Water Reactors, The Minerals, Metals & Materials Society, ISBN 978-3-319-67243-4, 2018, 973-991.
20. D. C. Johnson, G. S. Was, “Novel Technique for Quantitative Measurement of Localized Stresses Near Dislocation Channel-Grain Boundary Interaction Sites in Irradiated Stainless Steel,” Proc. 18th International Conference on Environmental Degradation of Materials in Nuclear Power Systems – Water Reactors, The Minerals, Metals & Materials Society, ISBN 978-3-319-67243-4, 2018, 1005-1013.
 21. J. R. Hesterberg, Z. Jiao, G. S. Was, “IASCC Susceptibility of 304L Stainless Steel Irradiated in a BWR and Subjected to Post Irradiation Annealing,” Proc. 18th International Conference on Environmental Degradation of Materials in Nuclear Power Systems – Water Reactors, The Minerals, Metals & Materials Society, ISBN 978-3-319-67243-4, 2018, 1015-1026.
 22. M. N. Gussev, G. S. Was, J. T. Busby, K. J. Leonard, “Plastic Deformation Processes Accompanying Stress Corrosion Crack Propagation in Irradiated Austenitic Steels,” Proc. 18th International Conference on Environmental Degradation of Materials in Nuclear Power Systems – Water Reactors, The Minerals, Metals & Materials Society, ISBN 978-3-319-67243-4, 2018, 1073-1084.
 23. R. D. Hanbury, G. S. Was, “Effect of Grain Orientation on Irradiation Assisted Corrosion of 31L Stainless Steel in Simulated PWR Primary Water,” Proc. 18th International Conference on Environmental Degradation of Materials in Nuclear Power Systems – Water Reactors, The Minerals, Metals & Materials Society, ISBN 978-3-319-67243-4, 2018, 1087-1096.
 24. A. M. Monterrosa, G. VanCoevering, Z. Jiao, G. S. Was, “The Influence of Bimodal Cavity Distributions on Swelling Evolution in Helium Pre-Implanted T91,” TMS Annual Meeting, Phoenix, AZ, March 2018.
 25. C. R. Lear, M. Song, M. Wang, G. S. Was, “Dual Ion Beam Irradiation of Commercial-Grade Austenitic Alloys Relevant to LWR Core Components at High Dose,” TMS Annual Meeting, Phoenix, AZ, March 2018.
 26. D. Woodley, Z. Jiao, K. Sun, G. S. Was, “Effect of Temperature and Helium on Microstructure Evolution in Dual Ion Irradiated HT9 Steel,” TMS Annual Meeting, Phoenix, AZ, March 2018.
 27. Z. Jiao, S. Taller, K. Field, G. S. Was, “Microstructure Evolution in BOR60-Irradiated T91,” TMS Annual Meeting, Phoenix, AZ, March 2018.
 28. G. VanCoevering, A. A. Kohnert, B. D. Wirth, G. S. Was, “A Heterogeneous Cavity Nucleation Model for Swelling in Simulated Ferritic Alloy,” TMS Annual Meeting, Phoenix, AZ, March 2018.
 29. J. Michalicka, Z. Jiao, G. S. Was, “Radiation-Induced Precipitates in a Self-Ion Irradiated Cold-Worked 316 Austenitic Stainless Steel Used for PWR Baffle-Bolts,” TMS Annual Meeting, Phoenix, AZ, March 2018.
 30. J. Hesterberg, J. J. Carter, R. W. Smith, G. S. Was, “Computer Simulations of Dislocation-Obstacle Interactions in the Hardness and Recovery of BWR-Irradiated 304L SS,” TMS Annual Meeting, Phoenix, AZ, March 2018.
 31. M. Wang, M. Song, X. Lou, R. B. Rebak, G. S. Was, “IASCC Behavior of Additively Manufactured 316L Stainless Steel in Light Water Reactor Environment,” TMS Annual Meeting, Phoenix, AZ, March 2018.

32. M. Song, M. Wang, G. S. Was, X. Lou, R. B. Rebak, "Effects of Proton Irradiation on Microstructure in Additively Manufactured 316L Stainless Steel Made by Laser Powder Bed Fusion," TMS Annual Meeting, Phoenix, AZ, March 2018.
33. P. Wang, G. S. Was, "Corrosion Products of FeCrAl Alloys in Simulated LWR Environments during In-Situ Proton Corrosion-Irradiation Experiment," TMS Annual Meeting, Phoenix, AZ, March 2018.
34. S. M. Leving, Z. Jiao, G. S. Was, "Using Ion Irradiation to Extend the Damage Level of Neutron Irradiated 304L Stainless Steel," TMS Annual Meeting, Phoenix, AZ, March 2018.
35. W. Kuang, G. S. Was, "The Effects of Grain Boundary Structure on the Intergranular Stress Corrosion Cracking Initiation Susceptibility of Alloy 690 in High Temperature Water," TMS Annual Meeting, Phoenix, AZ, March 2018.
36. S. Taller, Z. Jiao, K. Field, G. S. Was, "Impact of Temperature on Microstructural Features using Dual Ion-Irradiation in T91 Steel," TMS Annual Meeting, Phoenix, AZ, March 2018.